

# **The role of metabolic reprogramming and mitochondria in the antiviral functions of plasmacytoid dendritic cells**

**PD 115776**

**Final report**

## **1. Regulation of type I interferon responses by mitochondria-derived reactive oxygen species in plasmacytoid dendritic cells**

**Background:** Under oxidative stress conditions the intracellular levels of reactive oxygen species (ROS) are elevated that by damaging different biological targets such as proteins, lipids or DNA can lead to a variety of pathologies. Although multiple mechanisms can generate ROS within the cells in vivo, the mitochondrial electron transport chain is assumed to be the major source of endogenous ROS. As a natural process, some electrons leave the electron transport chain and react with molecular oxygen leading to the formation of mitochondrial ROS (mtROS), the natural byproducts of oxidative metabolism. An extensive body of literature indicates the involvement of mtROS in multiple signaling pathways including antiviral responses, which is in the focus of our project. However, the putative regulatory role of mtROS on signaling induced by antiviral sensors of plasmacytoid dendritic cells (pDCs) has not been investigated yet.

**Results:** In this project we have investigated the regulation of antiviral signaling by increased mtROS production in pDCs, which, as major producers of type I interferons (IFN), are the key coordinators of antiviral immunity. The early phase of type I IFN production in pDCs is mediated by endosomal TLRs, whereas the late phase of IFN response can also be triggered by cytosolic retinoic acid-inducible gene-I (RIG-I), expression of which is induced upon Toll-like receptor (TLR) stimulation. Therefore, pDCs provide an ideal model to study the impact of elevated mtROS on the antiviral signaling pathways initiated by receptors with distinct subcellular localization. We found that elevated level of mtROS alone did not change the phenotype and the baseline cytokine profile of resting pDCs. Nevertheless increased mtROS levels in pDCs lowered the TLR9-induced secretion of pro-inflammatory mediators slightly, whereas reduced type I IFN production markedly via blocking phosphorylation of interferon regulatory factor 7 (IRF7), the key transcription factor of the TLR9 signaling pathway. The TLR9-induced expression of RIG-I in pDCs was also negatively regulated by enhanced mtROS production. On the contrary, elevated mtROS significantly augmented the RIG-I-stimulated expression of type I IFNs, as well as the expression

of mitochondrial antiviral-signaling protein and the phosphorylation of Akt and IRF3 that are essential components of RIG-I signaling.

**Conclusion:** In conclusion, we propose a model where mtROS impact the TLR-induced first wave of type I IFN responses negatively, whereas affect the RIG-I-mediated second wave of type I IFN production positively. The opposing effect of mtROS on the TLR- and RIG-I-like receptor (RLR)-mediated signaling pathway reflects the versatile role of mtROS in fine-tuning the type I IFN mediated innate immune responses by pDCs. Further characterization of this spatio-temporal regulation of signaling pathways by mtROS might expand our knowledge to improve drugs targeting mtROS-dependent molecules for the treatment of inflammatory diseases.

*Zsofia Agod, Tünde Fekete, Marietta M. Budai, Aliz Varga, Attila Szabo, Hyelim Moon, Istvan Boldogh, Tamas Biro, Arpad Lanyi, Attila Bacsi, and Kitti Pazmandi. Regulation of type I interferon responses by mitochondria-derived reactive oxygen species in plasmacytoid dendritic cells. Redox Biol. 2017 Oct; 13: 633–645. doi: 10.1016/j.redox.2017.07.016*

## **2. Regulatory NLRs control the RLR-mediated type I interferon and inflammatory responses in human dendritic cells**

**Background:** DCs, acting as sentinels of the immune system, recognize various molecular motifs within pathogens through their pattern recognition receptors (PRRs) and rapidly produce inflammatory cytokines and/or antiviral molecules to initiate innate immune responses. In order to fulfil this task, DCs are equipped with an arsenal of germ-line encoded PRRs including TLRs, RLRs and nucleotide-binding domain leucine-rich repeat (NLRs). Recent evidence indicates that these PRRs might collaborate synergistically to counteract the infectious agents or antagonistically to attenuate overzealous inflammation.

In the first year of the project we observed that elevated mtROS production can regulate the antiviral responses of pDCs. According to these results we wanted to further investigate the mitochondria-associated regulatory processes in pDCs. In other cell types it has already described that mitochondria-targeted NLRs such as NLRX1 or NLRC5 can control the production of type I IFN responses induced by RIG-I/ MAVS signaling pathway activity. Moreover NLRX1 is able to influence the inflammatory responses of the cells via the regulation of mtROS production. However the role of these NLRs in the mitochondria-associated antiviral activity of pDCs has not been investigated yet. Our goal was to explore the expression profile of these mitochondria-targeted

regulatory NLRs and to reveal their contribution to the RLR-mediated cytokine responses in human pDCs as well as in human conventional DCs (cDCs).

**Results:** Plasmacytoid DCs, the most powerful type I IFN producing cells, preferentially employ endosomal TLRs to elicit antiviral IFN responses. By contrast, cDCs predominantly use cytosolic RLRs, which are constitutively expressed in them, to sense foreign nucleic acids. Previously we have reported that, though RIG-I is absent from resting pDCs, it is inducible upon TLR stimulation. In this study we investigated the regulatory ability of mitochondria-targeted NLRs, namely NLRC5 and NLRX1 directly associated with the RLR-mediated signaling pathway in DC subtypes showing different RLR expression, particularly in pDCs and monocyte-derived DCs (moDCs). We demonstrated that similarly to RLRs, NLRC5 is also inducible upon TLR9 stimulation, whereas NLRX1 is constitutively expressed in pDCs. Inhibition of NLRC5 and NLRX1 expression in pDCs augmented the RLR-stimulated expression of type I IFNs but did not affect the production of the pro-inflammatory cytokines TNF, IL-6 and the chemokine IL-8. Further we showed that immature moDCs constantly express RLRs, NLRX1 and NLRC5 that are gradually upregulated during their differentiation. Similarly to pDCs, NLRX1 suppression increased the RLR-induced production of type I IFNs in moDCs. Interestingly, RLR stimulation of NLRX1-silenced moDCs led to a significant increase in pro-inflammatory cytokine production and I $\kappa$ B $\alpha$  degradation, suggesting increased NF- $\kappa$ B activity. On the contrary, NLRC5 did not seem to have any effect on the RLR-mediated cytokine responses in moDCs.

**Conclusion:** Our work demonstrated that RLR-mediated innate immune responses are primarily regulated by NLRX1 and partly controlled by NLRC5 in human DCs. Accumulating evidence suggest that aberrant IFN production due to abnormal RLR activation is associated with the development of autoimmune diseases. Therefore, understanding the molecular mechanisms underlying the negative regulation of innate immunity might contribute to the development of effective therapies for inflammation-induced autoimmune diseases. From another aspect, these mitochondria-targeted regulatory NLRs working as molecular breaks on antiviral signaling might serve as potential therapeutic targets for enhancing host responses to pathogenic infection.

*Tünde Fekete, Dóra Bencze, Attila Szabo, Eszter Csoma, Tamas Biro, Attila Bacsi and Kitti Pázmándi. Regulatory NLRs control the RLR-mediated type I interferon and inflammatory responses in human dendritic cells. Front Immunol. 2018 Sept. doi: 10.3389/fimmu.2018.02314*

### **3. Human plasmacytoid and monocyte-derived dendritic cells display distinct metabolic profile upon RIG-I activation**

**Background:** A growing body of evidence indicates that the activation of DCs does not only trigger changes in the expression of genes associated with immune responses but also induce metabolic reprogramming, which is important to meet the energetic needs of DC activation.

Recent evidence indicates that activation of conventional DCs and macrophages is accompanied by rapid induction of glycolysis that provides adequate energy for activation and cytokine production. Our goal was to characterize the metabolic changes in pDCs in response to various activation signals. In the second year of the project our preliminary results showed that different ligands (CpG-A and CpG-B) of endosomal TLR9 resulted in the activation of distinct metabolic transition in pDCs. Unfortunately we were unable to validate these results with real-time extracellular flux analysis. Due to this reason we changed our strategy in the last year of the project and submitted a request to Professor László Acsádi, president of the National Research, Development and Innovation Office to transfer costs for essential reagents and isolation kits. After that our primary goal was to address the link between cellular metabolism and RLR-mediated signal transduction in human DCs. As far as we know there are no data in the literature concerning the metabolic adaptation of DCs in response to RLR stimulation. We also wanted to describe the differences between the TLR-driven and RLR-induced metabolic alterations of pDCs and aimed to compare the metabolic requirements of RIG-I stimulated human pDCs and moDCs displaying distinct viral sensing machinery and different cytosolic RIG-I expression profile. To sense viruses and trigger an early type I IFN response, pDCs rely on endosomal TLRs, whereas cDCs employ cytosolic RIG-I, which is constitutively present in their cytoplasm. However RIG-I is upregulated in pDCs upon endosomal TLR activation and contributes to the late phase of type I IFN responses.

**Results:** Our results demonstrated that TLR9-driven activation of human pDCs led to a metabolic transition to glycolysis supporting the production of type I IFNs, whereas RIG-I-mediated antiviral responses of pDCs did not require glycolysis and rather relied on oxidative phosphorylation (OXPHOS) activity. In particular, TLR9-activated pDCs showed increased extracellular acidification rate (ECAR), lactate production and upregulation of key glycolytic genes indicating an elevation in glycolytic flux. Furthermore, administration of 2-deoxy-D-glucose (2-DG), an inhibitor of glycolysis, significantly impaired the TLR9-induced secretion of type I IFNs by human pDCs. In contrast, RIG-I stimulation of pDCs did not result in any alterations of ECAR, and type

I IFN production was not inhibited but rather promoted by 2-DG treatment. Moreover, pDCs activated via TLR9 but not RIG-I in the presence of 2-DG were impaired in their capacity to prime naïve CD8<sup>+</sup> T cell proliferation. Interestingly, human moDC triggered via RIG-I showed a commitment to glycolysis to promote type I IFN production and T cell priming in contrast to pDCs.

**Conclusion:** In conclusion we showed that different DC subtypes such as human pDCs and moDCs have distinct metabolic requirements. In response to RIG-I stimulation moDCs switch to glycolysis whereas pDCs seems to rely on OXPHOS rather than glycolysis. These differences might be explained by the fact that these two DC subtypes possess different viral sensor repertoire which elicit divergent antiviral responses. Plasmacytoid DCs apply endosomal TLRs in the early phases of virus infection and use RIG-I only in the later stages of antiviral responses. On the contrary, moDCs engage both TLRs and RLRs during the initial viral encounter which, as we suppose, requires a switch to glycolysis to expand endoplasmic reticulum and Golgi for the large-scale production of antiviral proteins. Furthermore, our data imply that cellular metabolism controls the T cell priming function of human DCs indicating that metabolic manipulation of DCs might be used to modulate their immune-polarizing properties as well.

*Tünde Fekete, Máté István Sütő, Dóra Bencze, Anett Mázló, Attila Szabo, Tamas Biro, Attila Bacsi and Kitti Pázmándi. Human plasmacytoid and monocyte-derived dendritic cells display distinct metabolic profile upon RIG-I activation. Under revision in Frontiers in Immunology. Manuscript ID: 414492 (uploaded on 17<sup>th</sup> of July 2018)*

Please find the submitted version of the manuscript below.

# Human plasmacytoid and monocyte-derived dendritic cells display distinct metabolic profile upon RIG-I activation

Tünde Fekete<sup>1</sup>, **Máté I. Sütő**<sup>1</sup>, Dóra Bencze<sup>1</sup>, Anett Mázló<sup>1,2</sup>, Attila Szabo<sup>1</sup>, Tamas Biro<sup>1</sup>, Attila Bacs<sup>1</sup>, Kitti Pázmándi<sup>3\*</sup>

<sup>1</sup>Department of Immunology, Faculty of Medicine, University of Debrecen, Hungary, <sup>2</sup>MTA-DE Cell Biology and Signaling Research Group, University of Debrecen, Hungary, <sup>3</sup>University of Debrecen, Hungary

*Submitted to Journal:*  
Frontiers in Immunology

*Specialty Section:*  
Molecular Innate Immunity

*Article type:*  
Original Research Article

*Manuscript ID:*  
414492

*Received on:*  
17 Jul 2018

*Frontiers website link:*  
[www.frontiersin.org](http://www.frontiersin.org)

Review

### *Conflict of interest statement*

The authors declare that the research was conducted in the absence of any commercial or financial relationships that could be construed as a potential conflict of interest

### *Author contribution statement*

KP and TF designed the research, performed experiments, analyzed and interpreted data and wrote the manuscript. MS, DB, AM and ASZ performed experiments and participated in data analysis. KP, AB and TB contributed with essential reagents. All authors reviewed and approved the manuscript.

### *Keywords*

plasmacytoid dendritic cell, dendritic cell, metabolic reprogramming, Glycolysis, RIG-I, TLR, type I interferon, antiviral response

### *Abstract*

Word count: 350

Recent advances reveal that metabolic reprogramming is required for adequate antiviral responses of dendritic cells (DCs) that possess the capacity to initiate both innate and adaptive immune responses. Several reports indicate that Toll-like receptor (TLR) stimulation of DCs is accompanied by a rapid induction of glycolysis; however, the metabolic requirements of retinoic-acid inducible gene I (RIG-I)-like receptor (RLR) activation have not defined either in conventional DCs (cDCs) or in plasmacytoid DCs (pDCs) that are the major producers of type I interferons (IFN) upon viral infections.

To sense viruses and trigger an early type I IFN response, pDCs rely on endosomal TLRs, whereas cDCs employ cytosolic RIG-I, which is constitutively present in their cytoplasm. We previously found that RIG-I is upregulated in pDCs upon endosomal TLR activation and contributes to the late phase of type I IFN responses. Here we report that TLR9-driven activation of human pDCs leads to a metabolic transition to glycolysis supporting the production of type I IFNs, whereas RIG-I-mediated antiviral responses of pDCs do not require glycolysis and rather rely on oxidative phosphorylation (OXPHOS) activity. In particular, TLR9-activated pDCs show increased extracellular acidification rate (ECAR), lactate production and upregulation of key glycolytic genes indicating an elevation in glycolytic flux. Furthermore, administration of 2-deoxy-D-glucose (2-DG), an inhibitor of glycolysis, significantly impairs the TLR9-induced secretion of type I IFNs by human pDCs. In contrast, RIG-I stimulation of pDCs does not result in any alterations of ECAR, and type I IFN production is not inhibited but rather promoted by 2-DG treatment. Moreover, pDCs activated via TLR9 but not RIG-I in the presence of 2-DG are impaired in their capacity to prime naïve CD8<sup>+</sup> T cell proliferation. Interestingly, human monocyte-derived DCs (moDC) triggered via RIG-I show a commitment to glycolysis to promote type I IFN production and T cell priming in contrast to pDCs.

Our findings reveal for the first time, that pDCs display a unique metabolic profile: TLR9-driven but not RIG-I-mediated activation of pDCs requires glycolytic reprogramming. Nevertheless, the metabolic signature of RIG-I-stimulated moDCs is characterized by glycolysis suggesting that RIG-I-induced metabolic alterations are rather cell type-specific and not receptor-specific.

### *Ethics statements*

(Authors are required to state the ethical considerations of their study in the manuscript, including for cases where the study was exempt from ethical approval procedures)

*Does the study presented in the manuscript involve human or animal subjects:* No

1           **Human plasmacytoid and monocyte-derived dendritic cells**  
2           **display distinct metabolic profile upon RIG-I activation**

3  
4  
5   **Tünde Fekete<sup>1</sup>, Mate Sütő<sup>1</sup>, Dora Bencze<sup>1</sup>, Anett Mázló<sup>1, 2</sup>, Attila Szabo<sup>1</sup>, Tamas Biro<sup>1</sup>,**  
6   **Attila Bacsı<sup>1</sup>, Kitti Pazmandi<sup>1\*</sup>**

7  
8  
9   <sup>1</sup>Department of Immunology, Faculty of Medicine, University of Debrecen, Debrecen,  
10 Hungary;

11   <sup>2</sup>MTA-DE Cell Biology and Signaling Research Group, University of Debrecen, Debrecen,  
12 Hungary

13  
14  
15   **\*Correspondence:**

16   Kitti Pazmandi

17   [pazmandikitti@yahoo.de](mailto:pazmandikitti@yahoo.de)

18  
19  
20  
21   **Number of words:** 7174

22   **Number of figures:** 8

23   **Number of Supplementary Figures:** 2  
24  
25

### 26 **ABSTRACT**

27

28         Recent advances reveal that metabolic reprogramming is required for adequate  
29 antiviral responses of dendritic cells (DCs) that possess the capacity to initiate both innate and  
30 adaptive immune responses. Several reports indicate that Toll-like receptor (TLR) stimulation  
31 of DCs is accompanied by a rapid induction of glycolysis; however, the metabolic  
32 requirements of retinoic-acid inducible gene I (RIG-I)-like receptor (RLR) activation have not  
33 defined either in conventional DCs (cDCs) or in plasmacytoid DCs (pDCs) that are the major  
34 producers of type I interferons (IFN) upon viral infections.

35         To sense viruses and trigger an early type I IFN response, pDCs rely on endosomal  
36 TLRs, whereas cDCs employ cytosolic RIG-I, which is constitutively present in their  
37 cytoplasm. We previously found that RIG-I is upregulated in pDCs upon endosomal TLR  
38 activation and contributes to the late phase of type I IFN responses. Here we report that  
39 TLR9-driven activation of human pDCs leads to a metabolic transition to glycolysis  
40 supporting the production of type I IFNs, whereas RIG-I-mediated antiviral responses of  
41 pDCs do not require glycolysis and rather rely on oxidative phosphorylation (OXPHOS)  
42 activity. In particular, TLR9-activated pDCs show increased extracellular acidification rate  
43 (ECAR), lactate production and upregulation of key glycolytic genes indicating an elevation  
44 in glycolytic flux. Furthermore, administration of 2-deoxy-D-glucose (2-DG), an inhibitor of  
45 glycolysis, significantly impairs the TLR9-induced secretion of type I IFNs by human pDCs.  
46 In contrast, RIG-I stimulation of pDCs does not result in any alterations of ECAR, and type I  
47 IFN production is not inhibited but rather promoted by 2-DG treatment. Moreover, pDCs  
48 activated via TLR9 but not RIG-I in the presence of 2-DG are impaired in their capacity to  
49 prime naïve CD8<sup>+</sup> T cell proliferation. Interestingly, human monocyte-derived DCs (moDC)  
50 triggered via RIG-I show a commitment to glycolysis to promote type I IFN production and T  
51 cell priming in contrast to pDCs.

52         Our findings reveal for the first time, that pDCs display a unique metabolic profile;  
53 TLR9-driven but not RIG-I-mediated activation of pDCs requires glycolytic reprogramming.  
54 Nevertheless, the metabolic signature of RIG-I-stimulated moDCs is characterized by  
55 glycolysis suggesting that RIG-I-induced metabolic alterations are rather cell type-specific  
56 and not receptor-specific.

57

58 *Keywords:* plasmacytoid dendritic cell, dendritic cell, metabolic reprogramming, glycolysis,  
59 RIG-I, TLR, type I interferon, antiviral response

60

### INTRODUCTION

DCs as part of the innate immune system constitute the first line of defense against viral infections playing a crucial role in both the recognition of foreign nucleic acids and subsequent triggering of antiviral responses (1). The innate immune response to viral infections is initiated when germ line-encoded pattern recognition receptors (PRRs) recognize specific viral molecular patterns (2). Upon binding to viral components, the main viral sensors such as endosomal TLRs and cytosolic RLRs induce signaling cascades that stimulate the rapid expression of genes encoding antiviral products like type I IFNs (3).

Plasmacytoid DCs are a rare subtype of DCs that are specialized in producing large amounts of type I IFNs in response to viruses (4). Unlike cDCs, pDCs are resistant to most viral infections and require a direct physical contact with infected cells or an uptake of virus-derived components released by them to successfully mount an antiviral state (5, 6). Plasmacytoid DCs are known to rely mainly on the endosomal TLR7 and TLR9 receptors to detect viral nucleic acids, whereas cDCs preferentially use cytosolic RLRs to recognize replicating viral RNA intermediates (2, 7). Intriguingly, recent findings including ours suggest that besides the TLR-mediated sensing of viral nucleic acids, RLRs are also involved in virus-triggered pDCs activation (8-11). We have recently found that RIG-I, a cytoplasmic sensor of viral RNA, is absent from quiescent pDCs but can be greatly upregulated upon endosomal TLR stimulation (8). Further we have proposed a model where endosomal TLRs mediate the first wave of type I IFN production while RIG-I contributes to the late phase of type I IFN responses in pDCs (8).

A growing body of evidence indicates that the activation of DCs does not only trigger changes in the expression of genes associated with immune responses but also induce metabolic reprogramming, which is important to meet the energetic needs of DC activation [reviewed in (12)]. Interestingly, to ensure optimal environment for replication, viruses also modulate host cellular metabolism inducing specific host metabolic pathways by distinct mechanisms (13). Various families of viruses have shown to alter core cellular metabolic pathways: most viruses induce glycolysis, whereas others induce fatty acid synthesis as well as glutaminolysis (14). In addition it has been recognized that there is a crosstalk between the immune system and cellular metabolism; immune cells can shift their metabolism in response to distinct microenvironmental stimuli e.g. viral infections (14). Recent evidence indicates that activation of DCs and macrophages is accompanied by rapid induction of glycolysis that provides adequate energy for activation and cytokine production [reviewed in (15)]. Moreover in cDCs a range of TLR agonists has been found to induce a metabolic switch from OXPHOS to glycolysis which supports fatty acid synthesis that is required for DC activation (16, 17). Regarding the metabolic signature of activated pDCs only few studies are available, that all focus on endosomal TLR-driven metabolic alterations of pDCs (18-20). In particular, human pDCs show enhanced glycolytic activity upon stimulation with TLR7 specific respiratory viruses such as Flu and RV-16 virus and the synthetic TLR7 agonist gardiquimod (20). In contrast, activation of mouse pDCs through endosomal TLR9 resulted in increased OXPHOS and fatty acid oxidation (18). Furthermore, the authors demonstrated that the metabolic transition regulated through an autocrine type I IFN signaling loop is also characterized by changes in lipid metabolism that partially depends on the nuclear receptor peroxisome proliferator-activated receptor alpha (PPAR $\alpha$ ) in murine pDCs (18). All these findings imply that the activation-induced metabolic reprogramming of DCs might depend on the origin and source of the cells, the type of receptors as well as the activation signals.

As far as we know there are no data in the literature concerning the metabolic adaptation of DCs in response to RLR stimulation. Hence the primary goal of the present study is to address the link between cellular metabolism and RLR-mediated signal

## Metabolic profile of RIG-I activation

111 transduction in human DCs. In particular, we sought to explore the metabolic signature of  
112 RIG-I-activated human pDCs. Furthermore we aimed to compare the metabolic requirements  
113 of RIG-I stimulated human pDCs and moDCs displaying distinct viral sensing machinery and  
114 different cytosolic RIG-I expression profile.  
115

In review

### 116 MATERIALS AND METHODS

117

#### 118 Cell line

119

120 The human plasmacytoid dendritic cell line GEN2.2 (21) (provided by Dr. Joel Plumas  
121 and Dr. Laurence Chaperot, Research and Development Laboratory, French Blood Bank  
122 Rhône-Alpes, Grenoble, France) was used in our experiments, which is deposited with the  
123 CNCM (French National Collection of Microorganism Cultures) under the number CNCMI-  
124 2938. GEN2.2 cells were grown on a layer of mitomycin C (Sigma-Aldrich, St. Louis, MO,  
125 USA)-treated murine MS5 feeder cells (Cat. No. ACC 441, Leibniz Institute DSMZ-German  
126 Collection of Microorganisms and Cell Cultures, Braunschweig, Germany) in RPMI 1640  
127 medium (Sigma-Aldrich) supplemented with 10% heat-inactivated FBS (Life Technologies  
128 Corporation, Carlsbad, CA, USA), 100 U/ml penicillin, 100 µg/ml streptomycin (both from  
129 Sigma-Aldrich) and 5% non-essential amino acids (Life Technologies Corporation). For  
130 experiments, the GEN2.2 cells were removed from the feeder layer and seeded on 24-well  
131 plates at a concentration of  $5 \times 10^5$  cells / 500 µl in complete RPMI 1640 medium (Sigma-  
132 Aldrich). Cell lines were grown and incubated at 37 °C in 5% CO<sub>2</sub>, at humidified atmosphere.

133

#### 134 Isolation and culturing of primary human cells

135

136 Human heparinized leukocyte-enriched buffy coats were obtained from healthy blood  
137 donors drawn at the Regional Blood Center of Hungarian National Blood Transfusion Service  
138 (Debrecen, Hungary) in accordance with the written approval of the Director of the National  
139 Blood Transfusion Service and the Regional and Institutional Ethics Committee of the  
140 University of Debrecen, Faculty of Medicine (Debrecen, Hungary).

141 Peripheral blood mononuclear cells (PBMC) were separated from buffy coats by  
142 Ficoll-Paque Plus (Amersham Biosciences, Uppsala, Sweden) gradient centrifugation.  
143 Monocytes were purified from PBMCs by positive selection using magnetic cell separation  
144 with anti-CD14-conjugated microbeads (Miltenyi Biotec, Bergish Gladbach, Germany)  
145 according to the manufacturer's instructions. Freshly isolated cells were seeded in 24-well cell  
146 culture plates at a density of  $1 \times 10^6$  cells/ml in RPMI 1640 medium (Sigma-Aldrich)  
147 supplemented with 10% heat-inactivated FBS, 2 mM L-glutamine, 100 U/ml penicillin, 100  
148 µg/ml streptomycin (all from Sigma-Aldrich), 80 ng/ml GM-CSF (Gentaur Molecular  
149 Products, London, UK) and 50 ng/ml IL-4 (PeproTech, Brussels, Belgium) for 5 days. On day  
150 2, the half of the culture media was replaced with fresh media and the same amounts of GM-  
151 CSF and IL-4 were added to the cell cultures. Cells were used for experiments on day 5, when  
152 cells display immature DC phenotype (DC-SIGN/CD209<sup>+</sup>, CD14, CD1a<sup>+</sup>).

153 Primary human pDCs were isolated from PBMCs by positive selection using the  
154 human CD304 (BDCA-4/Neuropilin-1) MicroBead Kit (Miltenyi Biotec) according to the  
155 manufacturer's instructions, then cultured in 96-well plates at a density of  $1 \times 10^5$  cells / 200 µl  
156 in RPMI 1640 medium (Sigma-Aldrich) supplemented with 10% heat-inactivated FBS (Life  
157 Technologies Corporation), 2 mM L-glutamine, 100 U/ml penicillin, 100 µg/ml streptomycin  
158 (all from Sigma-Aldrich), and 50 ng/ml recombinant human IL-3 (PeproTech).

159 Naïve CD8<sup>+</sup> T cells were isolated from PBMC using the human naïve CD8<sup>+</sup> T cell  
160 isolation kit (Miltenyi Biotec) according to the manufacturer's instructions and were used for  
161 co-culture experiments as described below.

162

#### 163 Cell stimulation

164

165 For TLR activation GEN2.2 cells and primary human pDCs were treated with TLR9

166 agonist CpG-A (ODN 2216, 1  $\mu$ M; Hycult Biotech, Uden, The Netherlands) for 12 hours. To  
167 induce RIG-I expression GEN2.2 cells and primary human pDCs were pre-treated with low  
168 dose of CpG-A (0.25  $\mu$ M) for 16 hours. Thereafter the cells were washed, re-seeded in fresh,  
169 complete RPMI 1640 medium and stimulated with 5'ppp-dsRNA (InvivoGen, San Diego,  
170 CA, USA), a specific agonist of RIG-I in complex with the transfection reagent LyoVec<sup>TM</sup>  
171 (InvivoGen), according to the manufacturer's recommendations. Briefly, 25  $\mu$ l of the 5'ppp-  
172 dsRNA-LyoVec<sup>TM</sup> complex containing 1  $\mu$ g/ml working concentration of the RIG-I ligand  
173 was added to the cells for the indicated time periods in all experiments. For moDCs, on day 5  
174 of the differentiation half of the culture medium was removed, replaced by fresh medium then  
175 cells were exposed to 5'ppp-dsRNA-LyoVec<sup>TM</sup> complexes for 12 hours. In parallel  
176 experiments cells were treated with indicated concentrations of the glycolysis inhibitor 2-  
177 deoxy-D-glucose (2-DG, Sigma-Aldrich) or OXPHOS inhibitor carbonylcyanide m-  
178 chlorophenylhydrazone (CCCP, Sigma-Aldrich).

179

### 180 **Determination of cell viability**

181

182 Cell viability was assessed by 7-aminoactinomycin-D (7-AAD; 10  $\mu$ g/ml; Sigma-  
183 Aldrich) staining for 15 minutes immediately before flow cytometric analysis. Fluorescence  
184 intensities were measured with FACS Calibur cytometer (Becton Dickinson, Franklin Lakes,  
185 NJ, USA) and data were analyzed with FlowJo software (TreeStar, Ashland, OR, USA).

186

### 187 **Quantitative real-time PCR**

188

189 Total RNA was isolated from  $5 \times 10^5$  cells using Tri reagent (Molecular Research  
190 Center, Inc., Cincinnati, OH, USA). 1  $\mu$ g of total RNA was treated with DNase I (Thermo  
191 Fisher Scientific, Waltham, MA, USA) to exclude amplification of genomic DNA then  
192 reverse transcribed into cDNA using the High Capacity cDNA RT Kit of Applied Biosystems  
193 (Foster City, CA, USA). Gene expression assays were purchased from Thermo Fisher  
194 Scientific for *IFNB*, *hexokinase 2 (HK2)*, *lactate dehydrogenase A (LDHA)*, *hypoxia-*  
195 *inducible factor 1-alpha (HIF1A)*, and from Integrated DNA Technologies (Coralville, IA,  
196 USA) for *IFNA1* and *PPIA* (cyclophilin A). Quantitative PCR was performed using the ABI  
197 StepOne Real-Time PCR System (Applied Biosystems) and cycle threshold values were  
198 determined using the StepOne v2.1 Software (Applied Biosystems). The relative amount of  
199 mRNA ( $2^{-\Delta CT}$ ) was obtained by normalizing to the *PPIA* (Integrated DNA Technologies)  
200 housekeeping gene in each experiment.

201

### 202 **Assessment of cytokine levels and lactic acid from the supernatants of cell cultures**

203

204 Cell culture supernatants were collected at the indicated time points and IFN- $\alpha$  and  
205 IFN- $\beta$  levels were measured by the VeriKine<sup>TM</sup> Human Interferon Alpha and Beta ELISA kits,  
206 respectively (PBL Interferon Sources, Piscataway, NJ, USA) according to the manufacturer's  
207 instructions. Lactate production of the cells was detected using the Glycolysis Cell-Based  
208 Assay Kit (Cayman Chemical, Ann Arbor, Michigan, USA) according to the manufacturer's  
209 instructions. Absorbance measurements were carried out by a Synergy HT microplate reader  
210 (Bio-Tek Instruments, Winooski, VT, USA) at 450 nm for cytokine detection and at 490 nm  
211 for lactate assay.

212

### 213 **Real-time extracellular flux analysis**

214

215 Human pDCs and moDCs were harvested, washed and resuspended in Agilent

## Metabolic profile of RIG-I activation

216 Seahorse XF Base Medium (pH 7.4; Agilent Technologies, Santa Clara, CA, USA)  
217 supplemented with 10 mM glucose, 2 mmol/L glutamine and 1% FBS and seeded onto Cell-  
218 Tak (Corning Inc., NY, USA)-coated Seahorse XF96 Cell Culture Microplates (Agilent  
219 Technologies) at a density of  $1.5 \times 10^5$  cells per well. Cells were incubated at 37°C in a CO<sub>2</sub>-  
220 free incubator for 1 hour before the experiments. Extracellular acidification rate (ECAR) and  
221 oxygen consumption rate (OCR) were measured simultaneously in real-time with a Seahorse  
222 XF96<sup>e</sup> Extracellular Flux Analyzer (EFA; Agilent Technologies). The compounds, CpG-A and  
223 5'ppp-dsRNA were added immediately before EFA measurements.  
224

### 225 **Detection of mitochondrial reactive oxygen species (mtROS)**

226  
227 Primary pDCs and moDCs were loaded with 5 μM MitoSox™ Red mitochondrial  
228 superoxide indicator (Life Technologies Corporation) and incubated for 10 min at 37 °C  
229 protected from light. Then cells were washed gently three times with warm PBS buffer  
230 (Sigma-Aldrich) to remove the excess fluorescent dye and plated in 96-well black polystyrene  
231 plate at a density of  $2 \times 10^5$  cells / 200 μl in RPMI 1640 medium (Sigma-Aldrich). Cells were  
232 then left untreated or stimulated with 5'ppp-dsRNA as described above. Fluorescence  
233 intensity of MitoSox™ Red was recorded at 580 nm by a Synergy HT microplate reader (Bio-  
234 Tek Instruments).  
235

### 236 **Western blotting**

237  
238 For western blotting  $5 \times 10^5$  cells were lysed in Laemmli buffer and then the protein  
239 extracts were resolved by SDS-PAGE using 10% polyacrylamide gel and electro-transferred  
240 to nitrocellulose membranes (Bio-Rad Laboratories GmbH, Munich, Germany). Non-specific  
241 binding sites were blocked with 5% non-fat dry milk diluted in TBS Tween buffer (50 mM  
242 Tris, 0.5 M NaCl, 0.05% Tween-20, pH 7.4). Membranes were probed with the anti-RIG-I  
243 (Cat. No. 4520, Cell Signaling, Danvers, MA, USA) and anti-beta-actin (Cat. No. sc-47778,  
244 Santa Cruz Biotechnology) primary antibodies. The bound primary antibodies were labeled  
245 with anti-mouse or anti-rabbit horseradish peroxidase-conjugated secondary antibodies (GE  
246 Healthcare, Little Chalfont, Buckinghamshire, UK) at a dilution of 1:5000 and 1:10000,  
247 respectively and were visualized by the ECL system using SuperSignal West Pico  
248 chemiluminescent substrate (Thermo Scientific, Rockford, IL, USA) and X-ray film exposure.  
249 Densitometric analysis of immunoreactive bands was performed using Image Studio Lite  
250 Software version 5.2 (LI-COR Biosciences, Lincoln, Nebraska USA).  
251

### 252 **T cell proliferation assay**

253  
254 Prior to co-culture with naïve CD8<sup>+</sup> T cells primary human pDCs were stimulated with  
255 CpG-A (1 μM) for TLR9 activation in the presence or absence of 2-DG for 6 hours. In  
256 parallel experiments, primary pDCs were pre-treated with CpG-A (0.25 μM) for 16 hours to  
257 induce RIG-I expression as described above then following thorough washing steps  
258 stimulated with the specific RIG-I ligand 5'ppp-dsRNA with or without 2-DG for 6 hours.  
259 Immature moDCs were plated and stimulated with 5'ppp-dsRNA for 6 hours in the presence  
260 or absence of glycolysis inhibitor. Following incubation activated DCs were washed twice  
261 with cell culture medium then co-cultured in 96-well U-bottom plate with allogeneic naïve  
262 CD8<sup>+</sup> T cells, which were previously labeled with 0.5 μM of carboxyfluorescein succinimidyl  
263 ester (CFSE; Invitrogen, Carlsbad, CA, USA), for 5 days in the presence of 1 μg/ml anti-  
264 human CD3 monoclonal antibody (BD Pharmingen) at a ratio of 1:10 (DC-T cell). After co-  
265 cultivation, fluorescence intensities of CFSE dye were detected in the FL1 (530±15 nm)

266 channel on a BD FACS Calibur flow cytometer (Becton Dickinson) and data were analyzed  
267 by FlowJo software (Treestar).

268

269 **Statistical analysis**

270

271 Multiple comparisons were performed using ANOVA, followed by Bonferroni *post*  
272 *hoc* test whereas two groups were compared with Student's unpaired *t* test. Data analyses  
273 were performed using GraphPad Prism v.6 software (GraphPad Software Inc., La Jolla, CA,  
274 USA). Differences were considered to be statistically significant at  $p < 0.05$ .

275

In review

276 **RESULTS**

277

278 **Plasmacytoid DCs display distinct RIG-I expression profile compared to moDCs**

279

280 Due to the limited number of pDCs in human peripheral blood we performed most of  
 281 our experiments on the human pDC cell line GEN2.2 that shares similar phenotypic and  
 282 functional properties with primary human pDCs (22, 23). Furthermore, our main findings  
 283 have been validated in primary human pDCs isolated from peripheral blood of healthy  
 284 volunteers. Besides we have used moDCs generated from human peripheral blood monocytes  
 285 *in vitro* as it serves as an ideal model for studying DC functionality (24). First we investigated  
 286 the expression profile of RIG-I in these DC subtypes. Previously we have published that  
 287 GEN2.2 cells require a pre-treatment with TLR9 agonist CpG-A to express the cytosolic RIG-  
 288 I receptor (25) as also shown in **Figure 1A,D** of the present study. Similarly to GEN2.2 cells  
 289 RIG-I is also absent from resting primary pDCs (8) but can be significantly upregulated upon  
 290 exposure to CpG-A (**Figure 1B,E**) showing a unique RIG-I expression profile in pDCs. On  
 291 the contrary, RIG-I was gradually upregulated during moDC differentiation, and was  
 292 constantly present in 5-day immature moDCs (**Figure 1C,F**). Therefore, these two DC  
 293 subtypes provide potential models to study the RIG-I-induced metabolic changes in cell types  
 294 with different RIG-I expression profile, namely in moDCs that constitutively express RIG-I  
 295 and in pDCs with inducible RIG-I expression.

296

297 **Inhibition of glycolysis influences the viability and RIG-I expression of GEN2.2 cells**

298

299 Growing data support the idea that activation of DCs with various TLR agonists is  
 300 coupled with a metabolic transition (17, 20). To investigate the role of glycolysis in pDC  
 301 activation, cells were treated with the potent glycolysis inhibitor 2-deoxy-D-glucose (2-DG).  
 302 First we titrated 2-DG to determine the optimal concentration that would be tolerated by  
 303 GEN2.2 cells. Our results show that low doses of 2-DG (1-5 mM) do not or only slightly (10  
 304 mM) affected cell viability, whereas higher doses (20-50 mM) were not tolerated by GEN2.2  
 305 cells (**Figure 2A,B**). Based on our dose-response curve we have decided to use 1, 5 and 10  
 306 mM of 2-DG to our further experiments which concentrations of 2-DG did not markedly  
 307 increase the ratio of 7-AAD positive cells in the cell cultures.

308 Investigating the impact of glycolysis blockade on RIG-I expression we found that 1  
 309 and 5 mM concentrations of 2-DG did not influence the CpG-A induced expression of RIG-I  
 310 in GEN2.2 cells, whereas 10 mM of 2-DG decreased its protein levels significantly (**Figure**  
 311 **2C,D**). These results indicate that the RIG-I expression can be controlled by glycolysis in  
 312 pDCs.

313

314 **TLR but not RLR stimulation requires a shift toward glycolysis to induce a robust type I**  
315 **IFN production in GEN2.2 cells**

316

317 Previously we have described that following recognition of viral nucleic acids the type  
 318 I IFN production of pDCs occurs in two waves (8). Endosomal TLRs mediate early type I IFN  
 319 production; whereas cytosolic RLRs induced by TLR stimulation substantially contribute to  
 320 the late phase of IFN responses. We sought to test the role of glycolysis in both the first and  
 321 second phase of type I IFN responses in human pDCs. First we used the TLR9 ligand CpG-A  
 322 (1  $\mu$ M) to induce early type I IFN production in GEN2.2 cells. Time-dependent analysis of  
 323 *IFNA1* expression shows a peak at 12 hours following CpG-A stimulation (**Figure 3A**);  
 324 therefore, we have studied the effect of glycolysis at this time point. Inhibition of glycolysis  
 325 by 2-DG interrupted the CpG-A induced expression of IFN- $\alpha$  in a dose-dependent manner

326 both at the mRNA and protein level indicating a critical role for glycolysis in these processes  
327 (**Figure 3B,C**). The glycolysis inhibitor applied alone did not induce type I IFN production at  
328 any of the used concentrations (data not shown); therefore we excluded those treatment  
329 conditions from subsequent experiments. Next we measured real-time ECAR, an indicator of  
330 glycolysis, and found that GEN2.2 cells increased their ECAR levels following CpG-A  
331 administration (**Figure 3D**). Consistent with this, the elevated lactate production of CpG-A-  
332 stimulated cells indicates an increase in glycolytic activity that could be inhibited by  
333 administration of 2-DG (**Figure 3E**). We have also analyzed the changes in the expression of  
334 key glycolytic genes in CpG-A-exposed GEN2.2 cells at the mRNA level and we found that  
335 *LDHA*, *HK2* and *HIF1A* are significantly upregulated upon exposure to CpG-A (**Figure 3F-**  
336 **H**). All these results indicate that endosomal TLR9 stimulation requires glycolysis to induce  
337 type I IFN secretion in GEN2.2 cells.

338 Next we asked whether pDC activation in response to RIG-I stimulation is also  
339 accompanied by a shift toward glycolysis. Therefore GEN2.2 cells were pre-treated with low  
340 dose of CpG-A (0.25  $\mu$ M) for 16 hours to induce the cytosolic expression of RIG-I then  
341 following thorough washing steps stimulated with the specific RIG-I agonist 5'ppp-dsRNA.  
342 We have previously developed and applied this method successfully to study RLR responses  
343 in pDCs since a pre-treatment with low dose of CpG-A does not result in cell exhaustion (8,  
344 25). The activation of pDCs with a RIG-I ligand causes a more rapid type I IFN response than  
345 the activation with a TLR9 ligand. *IFNA1* mRNA expression peaks at 3 hours after RIG-I  
346 stimulation thus we have studied the impact of glycolysis inhibition at this early time point  
347 (**Figure 4A**). Interestingly, disruption of glycolysis by 2-DG significantly increased the  
348 5'ppp-dsRNA-induced expression of IFN- $\alpha$  both at the mRNA and protein level (**Figure**  
349 **4B,C**). Further we found that pDC activation in response to 5'ppp-dsRNA was not  
350 accompanied by an increase in ECAR (**Figure 4D**) in contrast to TLR9 activation. These  
351 results were supported by the findings that RIG-I stimulation did not give rise to elevated  
352 lactate production (**Figure 4E**) or upregulation of glycolysis-associated genes (**Figure 4F-H**).  
353 All these results imply that RIG-I-mediated type I IFN responses do not depend on glycolysis  
354 and instead use other metabolic pathways to ensure energy for the production of late type I  
355 IFN secretion.

356 In parallel experiments after the pre-treatment with low dose of CpG-A (0.25  $\mu$ M) we  
357 used high dose of CpG-A (1  $\mu$ M) instead of RIG-I ligand as a second stimulus to exclude the  
358 possibility that a preceding activation modifies the metabolic requirements to a subsequent  
359 stimulus. Here we observed that re-stimulation with CpG-A also requires glycolysis to induce  
360 IFN- $\alpha$  production in GEN2.2 cells (**Figure 5**). Particularly, blockade of glycolysis by 2-DG  
361 dampened IFN- $\alpha$  expression both at the mRNA and protein level following re-stimulation  
362 with CpG-A (**Figure 5A,B**). Furthermore, a second stimulus with CpG-A increased lactate  
363 production, which was inhibited by 2-DG administration (**Figure 5C**), and upregulated  
364 *LDHA*, *HK2* and *HIF1A* mRNA levels significantly (**Figure 5D-F**). All these results suggest  
365 that enhanced glycolysis dominates both early and late TLR9 responses, whereas RIG-I-  
366 mediated signaling does not rely on it in GEN2.2 cells.

### 367 368 **TLR but not RLR stimulation enhances glycolysis to induce the production of type I** 369 **IFNs even in primary human pDCs**

370  
371 To confirm our results we have also repeated our experiments with primary human  
372 pDCs. Due to the limited cell number only one concentration of 2-DG (5 mM) was tested that  
373 did not alter cell viability neither of GEN2.2 cells (**Figure 2A,B**) nor of primary pDCs  
374 (**Figure 6C,F**). Our results are in line with the data obtained by studies on the GEN2.2 cell  
375 line. The CpG-A-induced IFN- $\alpha$  production of primary pDCs was impaired in the presence of

376 2-DG (**Figure 6A**), whereas RIG-I-mediated IFN- $\alpha$  secretion was rather further increased in  
377 the presence of the glycolysis inhibitor (**Figure 6D**). Further we observed elevated lactate  
378 production in the supernatants of CpG-A stimulated cells that was reduced when cells were  
379 co-treated with 2-DG (**Figure 6B**). On the contrary, we did not observe any changes in the  
380 lactate levels of RIG-I stimulated pDCs (**Figure 6E**) indicating that RIG-I activation does not  
381 engage glycolysis and might use different metabolic pathways to serve  
382 macromolecule/protein synthesis.

383 In order to further investigate the metabolic signature of RIG-I stimulated GEN2.2  
384 cells and primary pDCs we wanted to study the importance of OXPHOS in RIG-I signaling.  
385 Therefore OXPHOS was uncoupled by the addition of potent OXPHOS inhibitor carbonyl  
386 cyanide m-chlorophenyl hydrazone (CCCP) (Figure S1 in Supplementary Material). First we  
387 determined the optimal concentrations (1, 5 and 10  $\mu$ M) of CCCP to treat GEN2.2 cells  
388 (Figure S1A,B in Supplementary Material), then observed that RIG-I-induced IFN- $\alpha$   
389 production of GEN2.2 cells was reduced in the presence of CCCP (Figure S1C,D in  
390 Supplementary Material). Performing real-time measurements of OCR in pDCs we observed  
391 a minimal increase in OCR upon RIG-I stimulation (Figure S1E in Supplementary Material).  
392 In primary human pDCs CCCP co-treatment also showed negative impact on the RIG-I  
393 induced IFN- $\alpha$  secretion (Figure S1F in Supplementary Material) without influencing the  
394 viability of the cells (Figure S1G in Supplementary Material). Furthermore, we detected  
395 elevated mtROS levels in primary pDCs after RIG-I activation (Figure S1H in Supplementary  
396 Material).

397 All these observations support the hypothesis that in contrast with TLR9 activation,  
398 human pDCs activated via RIG-I do not require glycolysis and might favor OXPHOS to  
399 produce type I IFNs.

400

### 401 Glycolysis is essential to the RIG-I-induced type I IFN production of moDCs

402

403 In order to test whether these results are specific to human pDCs we extended our  
404 studies on immature moDCs, which constantly express RIG-I in their resting state. First we  
405 tested the effects of 2-DG on the viability of moDCs. We have found that in contrast to pDCs  
406 moDCs tolerate all applied doses of 2-DG (1-50 mM) (**Figure 7A,B**). For better comparison,  
407 to our further experiments we used those 2-DG concentrations (1, 5 and 10 mM) which were  
408 also effective in pDCs.

409 In the next step we observed the maximal expression of mRNA for IFN- $\beta$ , the major  
410 type I IFN produced by moDCs, at 12 hours in response to RIG-I stimulation (**Figure 7C**),  
411 therefore we have studied the effects of glycolysis at this time point. Next we evaluated the  
412 impact of 2-DG on the RIG-I-stimulated IFN- $\beta$  expression at 12 hours and found that both the  
413 mRNA and protein levels of IFN- $\beta$  are dampened by the inhibition of glycolysis. (**Figure**  
414 **7D,E**). We also examined the metabolic profile of RIG-I stimulated moDCs in real-time and  
415 found a rapid increase in ECAR (**Figure 7F**) and decrease in OCR (Figure S2E in  
416 Supplementary Material) in contrast to pDCs (**Figure 4D** and Figure S1E in Supplementary  
417 Material). Lactate levels and the expression of key glycolytic genes (*LDHA*, *HK2* and *HIF1A*)  
418 were also elevated following RIG-I stimulation of moDCs suggesting increased glycolytic  
419 activity (**Figure 7G-J**). On the contrary, moDCs were less sensitive to CCCP treatment than  
420 pDCs (Figure S2A,B in Supplementary Material). Furthermore co-treatment of moDCs with  
421 specific RIG-I ligand and CCCP, did not alter significantly the type I IFN production as  
422 compared to moDCs treated with RIG-I ligand alone (Figure S2C,D in Supplementary  
423 Material). Moreover, the RIG-I ligand-exposed moDCs did not display increased mtROS  
424 production (Figure S2F in Supplementary Material). All these results indicate that in contrast  
425 to pDCs, activation of moDCs via RIG-I results in a metabolic switch from OXPHOS to

426 glycolysis.

427

428 **TLR9-stimulated primary human pDCs and RIG-I-activated moDCs but not RIG-I-**  
429 **stimulated pDCs require glycolytic metabolism to induce naïve T cell proliferation**

430

431 The transition of DCs from a quiescent into an activated state requires metabolic  
432 changes that might also shape their capacity to activate T cells (26). In the present study we  
433 have also investigated the impact of metabolism on the capacity of human DCs to interact  
434 with T cells. Therefore highly purified naïve CD8<sup>+</sup> T cells were co-cultured with primary  
435 human pDCs as well as moDCs (**Figure 8**). Prior to co-culturing, pDCs were stimulated with  
436 CpG-A or 5'ppp-dsRNA, and moDCs were also exposed to RIG-I ligand in the presence or  
437 absence of 5 mM 2-DG or left untreated for 6 hours.

438 Our results show that pDCs treated with TLR9 ligand CpG-A alone induce  
439 significant T cell proliferation which process was inhibited when pDCs were activated in the  
440 presence of 2-DG (**Figure 8A,D**). On the contrary, RIG-I-stimulated pDCs induced  
441 substantial T cell proliferation which was not influenced by 2-DG treatment of pDCs (**Figure**  
442 **8B,E**). However activation of moDCs with specific RIG-I ligand 5'ppp-dsRNA increased  
443 their T cell priming capacity which was significantly impaired upon co-treatment with 2-DG  
444 (**Figure 8C,F**). These observations suggest that the glycolysis in CpG-A-activated pDCs and  
445 RIG-I-stimulated moDCs is essential to induce the proliferation of CD8<sup>+</sup> T cell whereas the T  
446 cell priming capacity of RIG-I stimulated pDCs does not depend on it.

447

In review

## DISCUSSION

DCs are a heterogeneous family of cells that play an essential role in detecting pathogens through a wide array of PRRs such as TLRs and RLRs (27, 28). Ligation of these receptors leads to DC activation characterized by profound changes in gene expression allowing the production of inflammatory mediators as well as the upregulation of costimulatory molecules and major histocompatibility complex (MHC) I and II (29, 30). All these newly acquired properties enable DCs to initiate local inflammation and prime T cell responses (30). A growing body of evidence indicates that stimulation of immune cells including DCs is accompanied by metabolic reprogramming that plays an integral role in their activation process (12, 31). In particular, in response to TLR agonist cDCs and moDCs switch from OXPHOS to glycolysis, the inhibition of which impairs their activation and survival (17, 32, 33). Nevertheless, divergent findings have been reported concerning the role of cellular metabolism in endosomal TLR-mediated pDC activation (18, 20). To our present knowledge, the plausible relation of cellular metabolism to RLR signaling has not been addressed yet, therefore, in this study, we focused on the metabolic profile of RIG-I-stimulated human pDCs.

It has first been described in tumor cells that a metabolic switch from OXPHOS to glycolysis occurs even under normoxic condition to meet energy requirements for cell growth (34). The phenomenon is known as the Warburg effect, which is assumed to be utilized similarly by T-cells to promote proliferation and differentiation into effector cells (35). In contrast, the adoption of Warburg mechanism by innate immune cells, including macrophages and DCs appears to support functional changes such as the secretion of cytokines (12).

The importance of glycolysis in TLR-mediated DC activation has first been recognized by Jantsch *et al.* in 2008 (33). They have reported that the TLR4-mediated activation of mouse bone marrow (BM)-derived DCs is highly dependent on glycolysis which is tightly controlled by HIF-1 $\alpha$ . Another study demonstrated that stimulation of mouse BM-derived DCs with TLR2, TLR4 and TLR9 ligands promotes aerobic glycolysis that is accompanied by a decrease in mitochondrial activity and OXPHOS (17). Furthermore, it was found that the metabolic switch is supported by the phosphatidylinositol 3-kinase (PI3K)/Akt signaling and inhibited by the adenosine monophosphate-activated protein kinase (AMPK), a regulator of OXPHOS and by the anti-inflammatory cytokine IL-10. In subsequent studies it has been revealed that the early TLR-driven glycolytic reprogramming of BM-derived DCs are mediated via TANK-binding kinase 1 (TBK1), I $\kappa$ B kinase  $\epsilon$  (IKK $\epsilon$ ) and Akt by promoting the association of the glycolytic enzyme HK2 to the mitochondria (26), whereas the long-term commitment to glycolysis is regulated by the mammalian target of rapamycin complex 1 (mTORC1) that induces the expression of HIF1 $\alpha$  and inducible nitric oxide synthase (iNOS) (36). Furthermore, the authors propose that the prolonged commitment to glycolysis is only a survival mechanism of iNOS expressing DCs, in which NO production inhibits the mitochondrial electron transport chain (36). Nevertheless, an early increase in glycolytic flux, when iNOS is not active yet, has been suggested to be essential to initiate DC activation in mice. This has been proven by the findings that 2-DG, that inhibits HK2 in the glycolytic pathway, prevented the TLR4-mediated maturation, cytokine and lactate production of mouse BM-derived DCs at early stages of activation (17, 26). Furthermore, it has been suggested that the rapid increase in glycolysis in TLR-activated DCs might serve the *de novo* synthesis of fatty acids from citrate to support the expansion of organelles required for cytokine/protein synthesis and secretion (26).

Similarly to mouse BM-derived DCs it has been shown that human pDCs also switch to glycolysis to perform antiviral functions (20). The exposure of human pDCs to ssRNA viruses and gardiquimod increased HIF-1 $\alpha$  protein expression and induced early glycolysis, whereas decreased OXPHOS activity. Moreover, blockade of glycolysis by 2-DG impaired

498 the TLR7-induced maturation and IFN- $\alpha$  secretion of human pDCs indicating the critical role  
499 of glycolysis in pDC antiviral responses. Another study demonstrated that under pathological  
500 condition such as imiquimod-induced contact dermatitis, stimulation of both human and  
501 murine pDCs with imiquimod resulted in a decrease in OCR and increase in ECAR, however  
502 this was not the case with other TLR7/8 agonist, such as gardiquimod or R848 (19). In this  
503 study, we show that activation of human pDCs with the TLR9 agonist CpG-A also leads to an  
504 increase in glycolysis as reflected by enhanced ECAR, increased production of lactate and  
505 upregulation of glycolytic genes. Moreover, TLR9-induced production of type I IFNs was  
506 significantly inhibited by 2-DG highlighting the critical role for glycolysis in the antiviral  
507 function of human pDCs. In contrast to our findings, Wu *et al.* reported that TLR9-driven  
508 activation of murine pDCs induced metabolic changes characterized by increased OXPHOS  
509 and fatty acid oxidation that was found to be dependent of type I IFNs (18). Furthermore, type  
510 I IFN applied alone was also capable to enhance OXPHOS and fatty acid oxidation in murine  
511 pDCs (18). Additionally, the authors observed increased basal OCR in pDCs stimulated by  
512 imiquimod and in BM-derived DCs activated with the TLR3/MDA5 ligand polyinosinic-  
513 polycytidylic acid (polyI:C) (18). On the contrary, *in vivo* stimulation of mouse DCs with  
514 polyI:C resulted in metabolic reprogramming towards aerobic glycolysis that has been found  
515 to be regulated by type I IFNs (16).

516 So far, to our knowledge, only one study addressed the connection between cellular  
517 metabolism and RLR-mediated signaling (37). The authors used various cell lines (e.g.  
518 HEK293, MEF, J774A.1) transfected with plasmids encoding RIG-I to their experiments and  
519 described that the RLR-mediated antiviral response requires OXPHOS activity in response to  
520 viral infection. In line with this finding, we observed that pDC activation through RIG-I was  
521 not accompanied with an increase in glycolysis. Furthermore, RIG-I-mediated production of  
522 IFN- $\alpha$  was increased by 2-DG, whereas reduced by CCCP, a chemical inhibitor of OXPHOS  
523 in human pDCs. Our observations are consistent with the report of Yoshizumi *et al.* showing  
524 that arresting OXPHOS activity by CCCP disrupts RLR-mediated signaling in HEK293 cells  
525 (37). We also observed a minimal increase in OCR upon RIG-I stimulation that further  
526 support the idea that RIG-I-stimulated human pDCs rely on OXPHOS to fulfill their function.

527 It is worth to mention that the low dose of CpG-A applied to induce RIG-I in pDCs  
528 does not induce type I IFN production, however can promote a shift toward glycolysis (data  
529 not shown). Nevertheless, we suppose based on our results that this glycolytic shift might be a  
530 transient change and pDCs can increase their OXPHOS activity upon RIG-I stimulation.

531 Studies on human moDCs revealed that immature and tolerogenic moDCs display  
532 metabolic signatures of OXPHOS, fatty acid oxidation and glycolysis, whereas mature  
533 moDCs show higher glycolytic rate mirrored by increased lactate production (32). In contrast  
534 to murine mature BM-derived DCs, where the switch leads to a total blockade of OXPHOS  
535 and thus shows a complete dependence on glycolysis for energy production and survival (36),  
536 mature human moDCs still display a limited OXPHOS activity that is able to provide energy  
537 (32). In line with our observations the authors found that 50 mM 2-DG resulted only in a  
538 slight decrease in cell viability indicating high metabolic adaptation for survival. Interestingly,  
539 mature and immature moDCs showed similar levels of iNOS expression and NO production  
540 suggesting that the TLR-induced decrease in mitochondrial activity is NO-independent in  
541 human moDCs (32) in contrast to mouse DCs (36). We found that, in contrast to pDCs,  
542 human moDCs stimulated via RIG-I increased lactate release, upregulated the expression of  
543 glycolytic related genes and displayed higher ECAR and reduced OCR. While CCCP  
544 treatment did not have any significant effects, blockade of glycolysis by 2-DG impaired  
545 significantly the IFN- $\beta$  production of moDC indicating a dependence on glycolytic  
546 metabolism rather than OXPHOS.

547 In addition, we observed remarkable differences between primary pDCs and moDCs

548 concerning their mtROS production as RIG-I stimulation increased mtROS levels only in  
549 pDCs but not in moDCs. Interestingly, blockade of glycolysis increased the RIG-I-triggered  
550 type I IFN secretion in pDCs, whereas decreased it in moDCs. These results imply that, in  
551 contrast to moDCs, the defect of glycolysis in pDCs promotes OXPHOS activity that can  
552 result in increased mtROS production. Previously we have described that elevated levels of  
553 mtROS support the RIG-I-mediated responses in pDCs (25), thus we hypothesize that this  
554 might be the reason behind the increased type I IFN production of pDCs co-treated with RIG-  
555 I ligand and glycolysis inhibitor.

556 So far, limited data are available concerning the impact of metabolism on the capacity  
557 of human DCs to interact with T cells. It has been reported that *in vivo* activation of murine  
558 DCs in the presence of 2-DG impaired their CD4<sup>+</sup> and CD8<sup>+</sup> T cell stimulatory capacity  
559 demonstrating a crucial role for TLR-induced glycolysis in the priming functions of DCs (26).  
560 Our data also suggest an essential role for glycolytic metabolism in the priming function of  
561 TLR9-activated human pDCs and RIG-I-stimulated moDCs. Interestingly, treatment of pDCs  
562 with 2-DG did not have any effect on the CD8<sup>+</sup> T cell priming capacity of RIG-I-stimulated  
563 pDCs. All these data suggest that the immunogenic capacity of different DC subtypes  
564 coincides with their divergent metabolic demands.

565 In conclusion we show that different DC subtypes such as human pDCs and moDCs  
566 have distinct metabolic requirements. In response to RIG-I stimulation moDCs switch to  
567 glycolysis whereas pDCs seems to rely on OXPHOS rather than glycolysis. These differences  
568 might be explained by the fact that these two DC subtypes possess different viral sensor  
569 repertoire which elicit divergent antiviral responses. Plasmacytoid DCs apply endosomal  
570 TLRs in the early phases of virus infection and use RIG-I only in the later stages of antiviral  
571 responses. On the contrary, moDCs engage both TLRs and RLRs during the initial viral  
572 encounter which, as we suppose, requires a switch to glycolysis to expand endoplasmic  
573 reticulum and Golgi for the large-scale production of antiviral proteins (26). Furthermore, our  
574 data imply that cellular metabolism controls the T cell priming function of human DCs  
575 indicating that metabolic manipulation of DCs might be used to modulate their immune-  
576 polarizing properties as well. Overall, altering human DC functionality through metabolic  
577 modulation requires a more comprehensive knowledge and understanding due to the  
578 complexity and diversity of antiviral responses induced by various PRRs.  
579

580 **AUTHOR CONTRIBUTIONS**

581  
582 KP and TF designed the research, performed experiments, analyzed and interpreted  
583 data and wrote the manuscript. MS, DB, AM and ASZ performed experiments and  
584 participated in data analysis. KP, AB and TB contributed with essential reagents. All authors  
585 reviewed and approved the manuscript.

586  
587 **CONFLICT OF INTEREST**

588  
589 The authors declare that the research was conducted in the absence of any commercial  
590 or financial relationships that could be construed as a potential conflict of interest.

591  
592 **ABBREVIATIONS**

593  
594 2-DG: 2-deoxy-D-glucose  
595 CCCP: carbonyl cyanide m-chlorophenyl hydrazone  
596 cDC: conventional DC  
597 DC: dendritic cell  
598 ECAR: extracellular acidification rate  
599 HIF1A: hypoxia-inducible factor 1-alpha  
600 HK2: hexokinase 2  
601 IFN: interferon  
602 LDHA: lactate dehydrogenase A  
603 moDC: monocyte-derived DC  
604 mtROS: mitochondrial reactive oxygen species  
605 OCR: oxygen consumption rate  
606 OXPHOS: oxidative phosphorylation  
607 pDC: plasmacytoid DC  
608 RIG-I: retinoic-acid inducible gene I  
609 RLR: RIG-I-like receptors  
610 TLR: Toll-like receptors

611  
612 **ACKNOWLEDGMENTS**

613  
614 GEN2.2 cells used in this study were generously provided by Joel Plumas and  
615 Laurence Chaperot of Research and Development Laboratory, EFS Rhône-Alpes, 29 Av  
616 Maquis du Gresivaudan, BP 35, 38701 La Tronche, France.

617 We thank Péter Bai, leader of the MTA-DE Lendület Laboratory of Cellular  
618 Metabolism (Department of Medical Chemistry, Faculty of Medicine, University of Debrecen,  
619 Debrecen, Hungary) for providing access to Seahorse XF96<sup>e</sup> Extracellular Flux Analyzer to  
620 perform real-time extracellular flux analysis.

621  
622 **FUNDING**

623  
624 This work was supported by the National Research, Development and Innovation  
625 Office (NKFIH, PD 115776 and PD\_16 120887 to KP). The work was also supported by  
626 GINOP-2.3.2-15-2016-00050 project (to TB and AB). The project is co-financed by the  
627 European Union and the European Regional Development Fund. The research was also  
628 financed by the EFOP-3.6.3-VEKOP-16-2017-00009 project (to KP and DB). KP was also  
629 supported by the János Bolyai Research Scholarship from the Hungarian Academy of

630 Sciences.  
631

In review

## 632 REFERENCES

- 633
- 634 1. J. Geginat, G. Nizzoli, M. Paroni, S. Maglie, P. Larghi, S. Pascolo, *et al.* Immunity to  
635 Pathogens Taught by Specialized Human Dendritic Cell Subsets. *Front Immunol*  
636 (2015) 6:527. doi:10.3389/fimmu.2015.00527
- 637 2. S. Akira, S. Uematsu, and O. Takeuchi. Pathogen recognition and innate immunity.  
638 *Cell* (2006) 124:783-801. doi:10.1016/j.cell.2006.02.015
- 639 3. M.R. Thompson, J.J. Kaminski, E.A. Kurt-Jones, and K.A. Fitzgerald. Pattern  
640 recognition receptors and the innate immune response to viral infection. *Viruses*  
641 (2011) 3:920-40. doi:10.3390/v3060920
- 642 4. M. Swiecki, and M. Colonna. The multifaceted biology of plasmacytoid dendritic  
643 cells. *Nat Rev Immunol* (2015) 15:471-85. doi:10.1038/nri3865
- 644 5. B. Webster, S. Assil, and M. Dreux. Cell-Cell Sensing of Viral Infection by  
645 Plasmacytoid Dendritic Cells. *J Virol* (2016) 90:10050-10053. doi:10.1128/JVI.01692-  
646 16
- 647 6. T. Frenz, L. Graalman, C.N. Detje, M. Doring, E. Grabski, S. Scheu, *et al.*  
648 Independent of plasmacytoid dendritic cell (pDC) infection, pDC triggered by virus-  
649 infected cells mount enhanced type I IFN responses of different composition as  
650 opposed to pDC stimulated with free virus. *J Immunol* (2014) 193:2496-503.  
651 doi:10.4049/jimmunol.1400215
- 652 7. A. Pichlmair, and C. Reis e Sousa. Innate recognition of viruses. *Immunity* (2007)  
653 27:370-83. doi:10.1016/j.immuni.2007.08.012
- 654 8. A. Szabo, Z. Magyarics, K. Pazmandi, L. Gopcsa, E. Rajnavolgyi, and A. Bacsı. TLR  
655 ligands upregulate RIG-I expression in human plasmacytoid dendritic cells in a type I  
656 IFN-independent manner. *Immunol Cell Biol* (2014) 92:671-8.  
657 doi:10.1038/icb.2014.38
- 658 9. D. Bruni, M. Chazal, L. Sinigaglia, L. Chauveau, O. Schwartz, P. Despres, *et al.* Viral  
659 entry route determines how human plasmacytoid dendritic cells produce type I  
660 interferons. *Sci Signal* (2015) 8:ra25. doi:10.1126/scisignal.aaa1552
- 661 10. N. Marr, T.I. Wang, S.H. Kam, Y.S. Hu, A.A. Sharma, A. Lam, *et al.* Attenuation of  
662 respiratory syncytial virus-induced and RIG-I-dependent type I IFN responses in  
663 human neonates and very young children. *J Immunol* (2014) 192:948-57.  
664 doi:10.4049/jimmunol.1302007
- 665 11. A.E. Stone, S. Giugliano, G. Schnell, L. Cheng, K.F. Leahy, L. Golden-Mason, *et al.*  
666 Hepatitis C virus pathogen associated molecular pattern (PAMP) triggers production  
667 of lambda-interferons by human plasmacytoid dendritic cells. *PLoS Pathog* (2013)  
668 9:e1003316. doi:10.1371/journal.ppat.1003316
- 669 12. E.J. Pearce, and B. Everts. Dendritic cell metabolism. *Nat Rev Immunol* (2015) 15:18-  
670 29. doi:10.1038/nri3771
- 671 13. J.J. Gonzalez Plaza, N. Hulak, G. Kausova, Z. Zhumadilov, and A. Akilzhanova. Role  
672 of metabolism during viral infections, and crosstalk with the innate immune system.  
673 *Intractable Rare Dis Res* (2016) 5:90-6. doi:10.5582/irdr.2016.01008
- 674 14. E.L. Sanchez, and M. Lagunoff. Viral activation of cellular metabolism. *Virology*  
675 (2015) 479-480:609-18. doi:10.1016/j.virol.2015.02.038
- 676 15. L.A. O'Neill, and E.J. Pearce. Immunometabolism governs dendritic cell and  
677 macrophage function. *J Exp Med* (2016) 213:15-23. doi:10.1084/jem.20151570
- 678 16. A. Pantel, A. Teixeira, E. Haddad, E.G. Wood, R.M. Steinman, and M.P. Longhi.  
679 Direct type I IFN but not MDA5/TLR3 activation of dendritic cells is required for  
680 maturation and metabolic shift to glycolysis after poly IC stimulation. *PLoS Biol*  
681 (2014) 12:e1001759. doi:10.1371/journal.pbio.1001759

- 682 17. C.M. Krawczyk, T. Holowka, J. Sun, J. Blagih, E. Amiel, R.J. DeBerardinis, *et al.*  
683 Toll-like receptor-induced changes in glycolytic metabolism regulate dendritic cell  
684 activation. *Blood* (2010) 115:4742-9. doi:10.1182/blood-2009-10-249540
- 685 18. D. Wu, D.E. Sanin, B. Everts, Q. Chen, J. Qiu, M.D. Buck, *et al.* Type 1 Interferons  
686 Induce Changes in Core Metabolism that Are Critical for Immune Function. *Immunity*  
687 (2016) 44:1325-36. doi:10.1016/j.immuni.2016.06.006
- 688 19. N. Garzorz-Stark, F. Lauffer, L. Krause, J. Thomas, A. Atenhan, R. Franz, *et al.* Toll-  
689 like receptor 7/8 agonists stimulate plasmacytoid dendritic cells to initiate TH17-  
690 deviated acute contact dermatitis in human subjects. *J Allergy Clin Immunol* (2018)  
691 141:1320-1333 e11. doi:10.1016/j.jaci.2017.07.045
- 692 20. G. Bajwa, R.J. DeBerardinis, B. Shao, B. Hall, J.D. Farrar, and M.A. Gill. Cutting  
693 Edge: Critical Role of Glycolysis in Human Plasmacytoid Dendritic Cell Antiviral  
694 Responses. *J Immunol* (2016) 196:2004-9. doi:10.4049/jimmunol.1501557
- 695 21. L. Chaperot, A. Blum, O. Manches, G. Lui, J. Angel, J.P. Molens, *et al.* Virus or TLR  
696 agonists induce TRAIL-mediated cytotoxic activity of plasmacytoid dendritic cells. *J*  
697 *Immunol* (2006) 176:248-55. doi:
- 698 22. P. Carmona-Saez, N. Varela, M.J. Luque, D. Toro-Dominguez, J. Martorell-Marugan,  
699 M.E. Alarcon-Riquelme, *et al.* Metagene projection characterizes GEN2.2 and CAL-1  
700 as relevant human plasmacytoid dendritic cell models. *Bioinformatics* (2017) 33:3691-  
701 3695. doi:10.1093/bioinformatics/btx502
- 702 23. J. Di Domizio, A. Blum, M. Gallagher-Gambarelli, J.P. Molens, L. Chaperot, and J.  
703 Plumas. TLR7 stimulation in human plasmacytoid dendritic cells leads to the  
704 induction of early IFN-inducible genes in the absence of type I IFN. *Blood* (2009)  
705 114:1794-802. doi:10.1182/blood-2009-04-216770
- 706 24. C. Qu, N.S. Brinck-Jensen, M. Zang, and K. Chen. Monocyte-derived dendritic cells:  
707 targets as potent antigen-presenting cells for the design of vaccines against infectious  
708 diseases. *Int J Infect Dis* (2014) 19:1-5. doi:10.1016/j.ijid.2013.09.023
- 709 25. Z. Agod, T. Fekete, M.M. Budai, A. Varga, A. Szabo, H. Moon, *et al.* Regulation of  
710 type I interferon responses by mitochondria-derived reactive oxygen species in  
711 plasmacytoid dendritic cells. *Redox Biol* (2017) 13:633-645.  
712 doi:10.1016/j.redox.2017.07.016
- 713 26. B. Everts, E. Amiel, S.C. Huang, A.M. Smith, C.H. Chang, W.Y. Lam, *et al.* TLR-  
714 driven early glycolytic reprogramming via the kinases TBK1-IKKvarepsilon supports  
715 the anabolic demands of dendritic cell activation. *Nat Immunol* (2014) 15:323-32.  
716 doi:10.1038/ni.2833
- 717 27. T. Kawai, and S. Akira. Toll-like receptors and their crosstalk with other innate  
718 receptors in infection and immunity. *Immunity* (2011) 34:637-50.  
719 doi:10.1016/j.immuni.2011.05.006
- 720 28. T. Kawai, and S. Akira. The role of pattern-recognition receptors in innate immunity:  
721 update on Toll-like receptors. *Nat Immunol* (2010) 11:373-84. doi:10.1038/ni.1863
- 722 29. A. Boltjes, and F. van Wijk. Human dendritic cell functional specialization in steady-  
723 state and inflammation. *Front Immunol* (2014) 5:131. doi:10.3389/fimmu.2014.00131
- 724 30. A. Agrawal, S. Agrawal, and S. Gupta. Role of Dendritic Cells in Inflammation and  
725 Loss of Tolerance in the Elderly. *Front Immunol* (2017) 8:896.  
726 doi:10.3389/fimmu.2017.00896
- 727 31. B. Everts, and E.J. Pearce. Metabolic control of dendritic cell activation and function:  
728 recent advances and clinical implications. *Front Immunol* (2014) 5:203.  
729 doi:10.3389/fimmu.2014.00203
- 730 32. F. Malinarich, K. Duan, R.A. Hamid, A. Bijin, W.X. Lin, M. Poidinger, *et al.* High  
731 mitochondrial respiration and glycolytic capacity represent a metabolic phenotype of

- 732 human tolerogenic dendritic cells. *J Immunol* (2015) 194:5174-86.  
733 doi:10.4049/jimmunol.1303316
- 734 33. J. Jantsch, D. Chakravorty, N. Turza, A.T. Prechtel, B. Buchholz, R.G. Gerlach, *et al.*  
735 Hypoxia and hypoxia-inducible factor-1 alpha modulate lipopolysaccharide-induced  
736 dendritic cell activation and function. *J Immunol* (2008) 180:4697-705. doi:  
737 34. O. Warburg, F. Wind, and E. Negelein. The Metabolism of Tumors in the Body. *J Gen*  
738 *Physiol* (1927) 8:519-30. doi:  
739 35. S. Koudhi, A.B. Elgaaied, and S. Chouaib. Impact of Metabolism on T-Cell  
740 Differentiation and Function and Cross Talk with Tumor Microenvironment. *Front*  
741 *Immunol* (2017) 8:270. doi:10.3389/fimmu.2017.00270
- 742 36. B. Everts, E. Amiel, G.J. van der Windt, T.C. Freitas, R. Chott, K.E. Yarasheski, *et al.*  
743 Commitment to glycolysis sustains survival of NO-producing inflammatory dendritic  
744 cells. *Blood* (2012) 120:1422-31. doi:10.1182/blood-2012-03-419747
- 745 37. T. Yoshizumi, H. Imamura, T. Taku, T. Kuroki, A. Kawaguchi, K. Ishikawa, *et al.*  
746 RLR-mediated antiviral innate immunity requires oxidative phosphorylation activity.  
747 *Sci Rep* (2017) 7:5379. doi:10.1038/s41598-017-05808-w  
748

In review

749 **FIGURES**

750

751 **Figure 1.** Plasmacytoid DCs display distinct RIG-I expression profile compared to moDCs.  
 752 GEN2.2 cells (**A,D**) and primary human pDCs (**B,E**) were treated with TLR9 agonist CpG-A  
 753 (0.25  $\mu$ M) for 16 hours then the protein level of RIG-I was determined by western blotting.  
 754 (**C,F**) Freshly isolated monocytes were seeded in 24-well plates and differentiated as  
 755 described in the Materials and Methods. The protein level of RIG-I was measured by western  
 756 blotting. Representative blots are shown in (**A**), (**B**) and (**C**). Data are shown as mean  $\pm$  SD of  
 757 at least 3 independent measurements in (**D**), (**E**), (**F**). \* $p$ <0.05, \*\* $p$ <0.01, \*\*\*\* $p$ <0.0001

758

759 **Figure 2.** Inhibition of glycolysis influences the viability and RIG-I expression of GEN2.2  
 760 cells in a concentration-dependent manner. (**A,B**) GEN2.2 cells were treated with increasing  
 761 concentration of 2-deoxy-D-glucose (2-DG; 1-50 mM) then cell viability was analyzed by  
 762 flow cytometry. (**C,D**) GEN2.2 cells were left untreated, treated with TLR9 ligand CpG-A  
 763 (0.25  $\mu$ M) alone or in combination with increasing concentrations of 2-DG (1-10 mM) for 16  
 764 hours then the protein level of RIG-I was measured by western blot. (**A**) Representative dot  
 765 plots are shown, where numbers indicate the percentage of 7-AAD negative cells. (**B**) Bar  
 766 graphs show the mean  $\pm$  SD of 4 independent experiments. (**C**) Representative blot is shown.  
 767 (**D**) Bar graphs represent the mean  $\pm$  SD of 4 individual experiments. \*\* $p$ <0.01, \*\*\* $p$ <0.01  
 768 \*\*\*\* $p$ <0.0001 vs. control; ## $p$ <0.01

769

770 **Figure 3.** A shift to glycolysis is essential to the CpG-A-induced production of type I IFNs in  
 771 GEN2.2 cells. (**A**) GEN2.2 cells were treated with 1  $\mu$ M of CpG-A, and the expression of  
 772 *IFNA1* was measured in a time-dependent manner at the mRNA level by Q-PCR. (**B,C**)  
 773 GEN2.2 cells were left untreated, treated with 1  $\mu$ M of CpG-A alone or in combination with  
 774 increasing concentrations of 2-deoxy-D-glucose (2-DG; 1-10 mM) for 12 hours. The IFN- $\alpha$   
 775 expression was assessed by real-time PCR at the mRNA level (**B**) and by ELISA at the protein  
 776 level (**C**). (**D**) Following activation with CpG-A real-time ECAR of GEN2.2 cells was  
 777 determined by EFA. The results of a representative experiment are shown. (**E**) Lactate  
 778 concentrations were measured from the supernatants at 12 hours. The expression of *LDHA*  
 779 (**F**), *HK2* (**G**) and *HIF1A* (**H**) was assessed at the mRNA level by real-time PCR. Figures  
 780 represent the mean  $\pm$  SD of 4-6 independent experiments. \* $p$ <0.05, \*\* $p$ <0.01, \*\*\* $p$ <0.01  
 781 \*\*\*\* $p$ <0.0001 vs. control; ### $p$ <0.001, #### $p$ <0.0001, ND: not determined

782

783 **Figure 4.** Glycolysis is not required to the RIG-I-mediated type I IFN production in GEN2.2  
 784 cells. (**A**) GEN2.2 cells were pre-treated with 0.25  $\mu$ M of CpG-A for 16 hours then following  
 785 thorough washing steps stimulated with the RIG-I agonist 5'ppp-dsRNA (RIGL, 1  $\mu$ g/ml) in a  
 786 time-dependent manner. The mRNA level of *IFNA1* was measured by Q-PCR. (**B,C**) After  
 787 pre-treatment with low dose of CpG-A, GEN2.2 cells were exposed to 5'ppp-dsRNA in the  
 788 absence or presence of the indicated concentrations of 2-deoxy-D-glucose (2-DG; 1-10 mM).  
 789 The IFN- $\alpha$  expression was assessed by real-time PCR at the mRNA level (**B**) and by ELISA at  
 790 the protein level (**C**). (**D**) Following activation with 5'ppp-dsRNA real-time ECAR of  
 791 GEN2.2 cells was determined by EFA. The results of a representative experiment are shown.  
 792 (**E**) Lactate levels were measured from the supernatants of the cell cultures. The expression of  
 793 *LDHA* (**F**), *HK2* (**G**), and *HIF1A* (**H**) was assessed at the mRNA level by real-time PCR. Data  
 794 represent the mean  $\pm$  SD of at least 3 independent experiments. \*\* $p$ <0.01, \*\*\* $p$ <0.01,  
 795 \*\*\*\* $p$ <0.0001 vs. control; # $p$ <0.05, ## $p$ <0.01, ### $p$ <0.001, #### $p$ <0.0001, ND: not determined

796

797 **Figure 5.** The type I IFN production of GEN2.2 cells induced by a second exposure to CpG-A  
 798 also depends on glycolytic metabolism. GEN2.2 cells were pre-treated with 0.25  $\mu$ M of CpG-

799 A for 16 hours then following thorough washing steps re-stimulated with 1  $\mu$ M CpG-A (re-  
 800 CpG-A) in the absence or presence of 2-deoxy-D-glucose (2-DG; 1-10 mM). The *IFNA1*  
 801 mRNA expression level was assessed by real-time PCR (A) and the IFN- $\alpha$  protein level was  
 802 measured by ELISA (B) at 12 hours. (C) Lactate concentrations were determined from the  
 803 supernatants of the cells at 12 hours. The expression of *LDHA* (D), *HK2* (E), and *HIF1A* (F)  
 804 was assessed at the mRNA level by real-time PCR. (A-F) Bar graphs represent the mean  $\pm$  SD  
 805 of 4 independent experiments. \* $p$ <0.05, \*\* $p$ <0.01, \*\*\*\* $p$ <0.0001 vs. control; # $p$ <0.05,  
 806 ## $p$ <0.01, ### $p$ <0.001, #### $p$ <0.0001, ND: not determined

807  
 808 **Figure 6.** TLR9 but not RIG-I activation requires glycolysis to induce the production of type I  
 809 IFNs in primary human pDCs. Freshly isolated primary human pDCs were stimulated with 1  
 810  $\mu$ M of CpG-A in the absence or presence of 2-deoxy-D-glucose (2-DG; 5 mM) then IFN- $\alpha$   
 811 protein levels (A) and lactate concentrations (B) were measured from the supernatants of the  
 812 cells at 12 hours. In parallel experiments cells were pre-treated with low dose of CpG-A for  
 813 16 hours then following thorough washing steps stimulated with 5'ppp-dsRNA (RIGL, 1  
 814  $\mu$ g/ml) alone or in combination with 5 mM of 2-DG or left untreated. IFN- $\alpha$  protein levels (D)  
 815 and lactate concentrations (E) were measured from the supernatants at 6 hours. (C,F) Cell  
 816 viability was measured by 7-AAD staining using flow cytometry. (A-F) Data represent the  
 817 mean  $\pm$  SD of 3 individual experiments. \* $p$ <0.05, \*\*\* $p$ <0.01 vs. control; # $p$ <0.05, ## $p$ <0.01,  
 818 ND: not determined

819  
 820 **Figure 7.** Glycolytic switch is required to the RIG-I-mediated type I IFN production in  
 821 moDCs. (A,B) Immature moDCs were treated with increasing concentration of 2-deoxy-D-  
 822 glucose (2-DG; 1-50 mM) then cell viability was analyzed by flow cytometry. (C) Immature  
 823 moDCs were stimulated with the RIG-I agonist 5'ppp-dsRNA (RIGL, 1  $\mu$ g/ml) in a time-  
 824 dependent manner. Kinetics expression of *IFNB* mRNA was measured by Q-PCR. (D,E) In  
 825 parallel experiments moDCs were treated with RIG-I ligand in the absence or in the presence  
 826 of the indicated concentrations of 2-deoxy-D-glucose (2-DG; 1-10 mM) for 12 hours. The  
 827 IFN- $\beta$  expression was assessed by real-time PCR at the mRNA level (D) and by ELISA at the  
 828 protein level (E). (F) Following activation with RIG-I agonist 5'ppp-dsRNA, real-time ECAR  
 829 of moDCs was determined by EFA. The results of a representative experiment are shown. (G)  
 830 Lactate concentrations were measured from the supernatants at 12 hours. The expression of  
 831 *LDHA* (H), *HK2* (I), and *HIF1A* (J) was assessed at the mRNA level by real-time PCR. (A)  
 832 Representative dot plots are shown where numbers indicate the percentage of 7-AAD  
 833 negative cells. (B-E,G-J) Data represent the mean  $\pm$  SD of 4 independent experiments.  
 834 \* $p$ <0.05, \*\* $p$ <0.01, \*\*\* $p$ <0.01, \*\*\*\* $p$ <0.0001 vs. control; # $p$ <0.05, ## $p$ <0.01, #### $p$ <0.0001,  
 835 ND: not determined

836  
 837 **Figure 8.** TLR9-stimulated primary human pDCs and RIG-I-activated moDCs but not RIG-I-  
 838 activated pDC require glycolytic metabolism to induce naïve T cell proliferation. (A-F)  
 839 CFSE-labeled naïve CD8<sup>+</sup> T cells were co-cultured with pDCs or moDCs pre-treated with the  
 840 indicated reagents. After 5 days of co-cultivation, cell division was measured by flow  
 841 cytometry. (A-C) Representative histograms are shown where numbers indicate the  
 842 percentage of viable dividing CD8<sup>+</sup> T cells. (D-F) Bar graphs represent the mean  $\pm$  SD of 4  
 843 independent experiments. \*\*\* $p$ <0.01, \*\*\*\* $p$ <0.0001 vs. control; ### $p$ <0.001, #### $p$ <0.0001, 2-  
 844 DG: 2-deoxy-D-glucose; ND: not determined, RIGL: RIG-I ligand

Figure 1.TIF

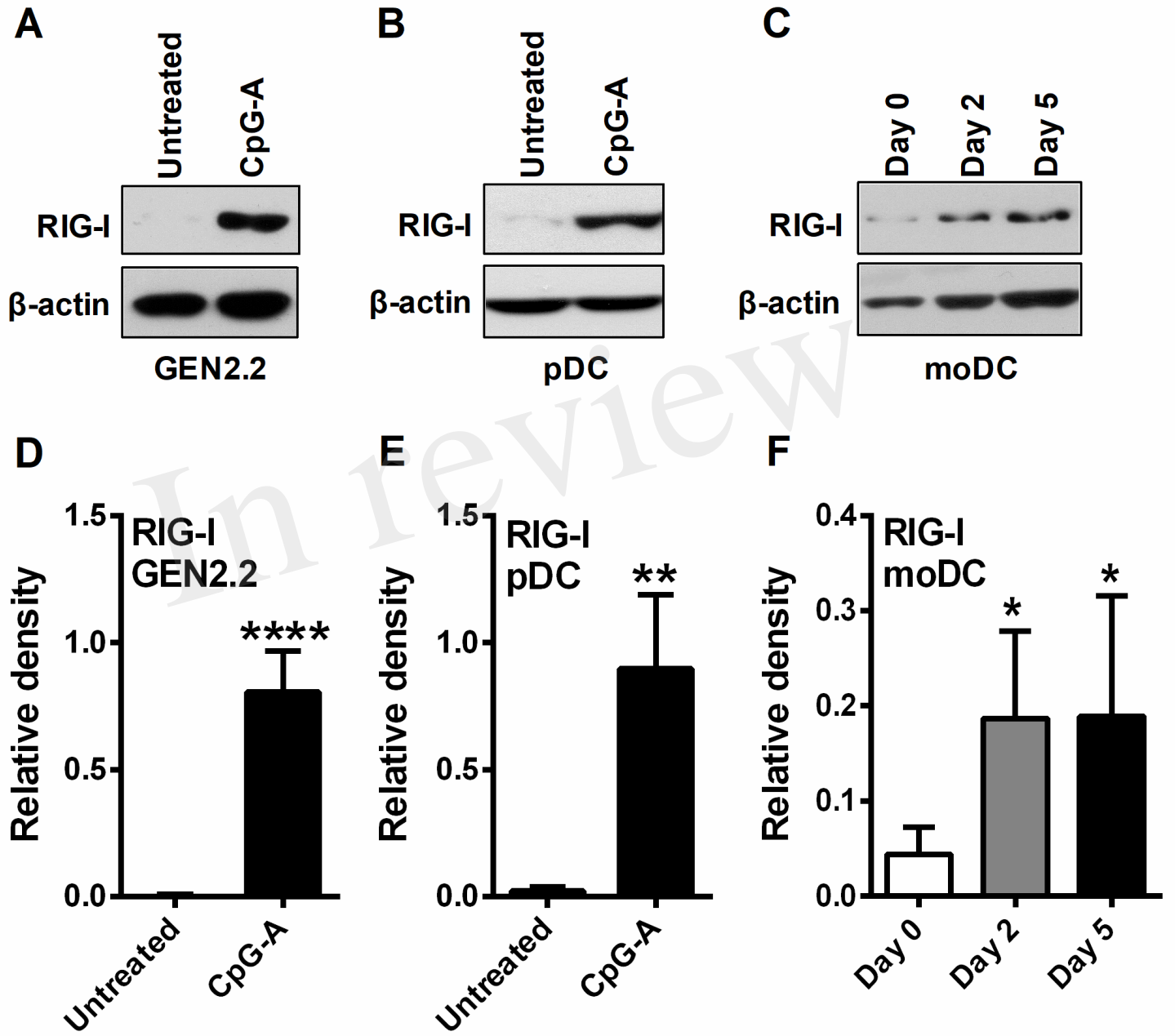


Figure 2.TIF

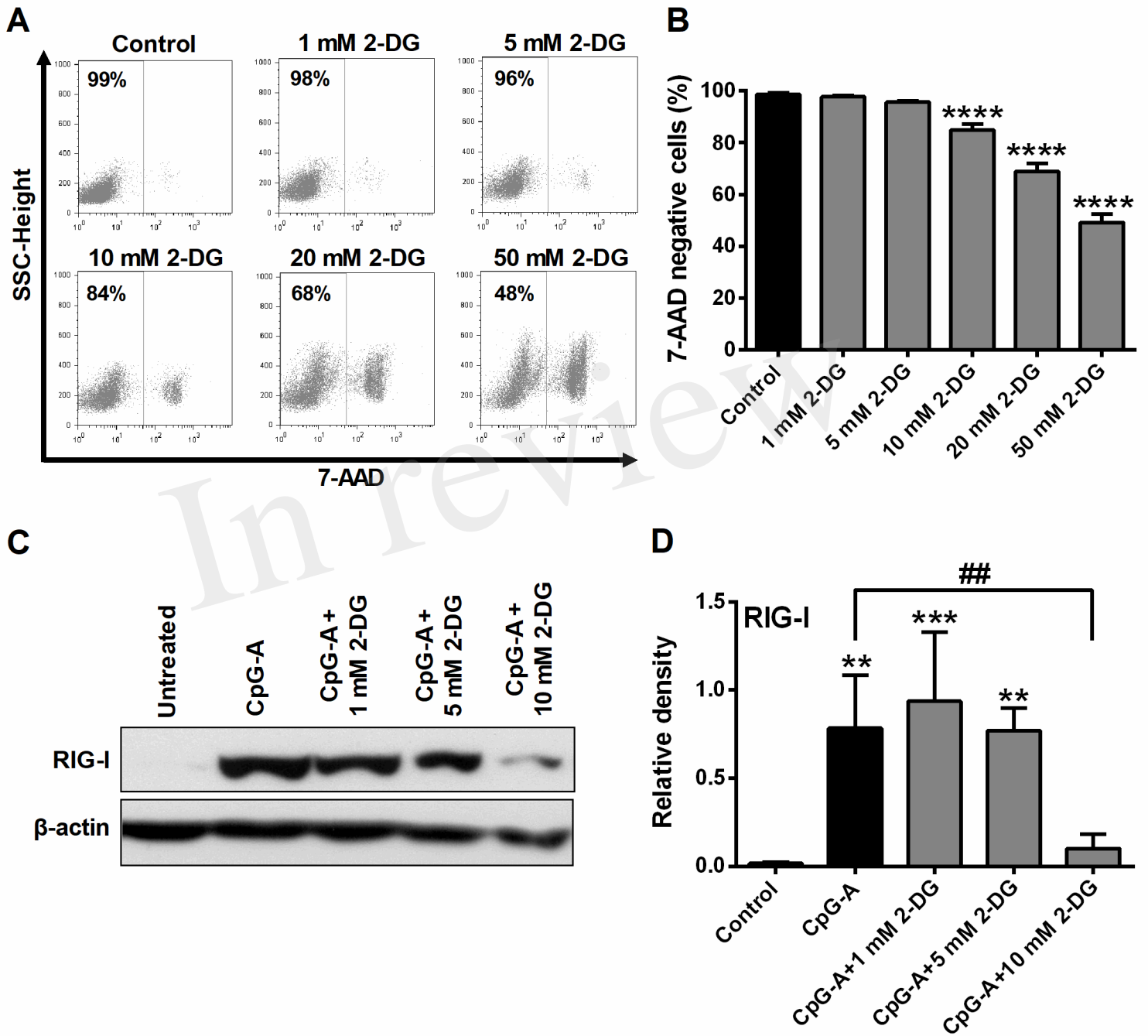


Figure 3.TIF

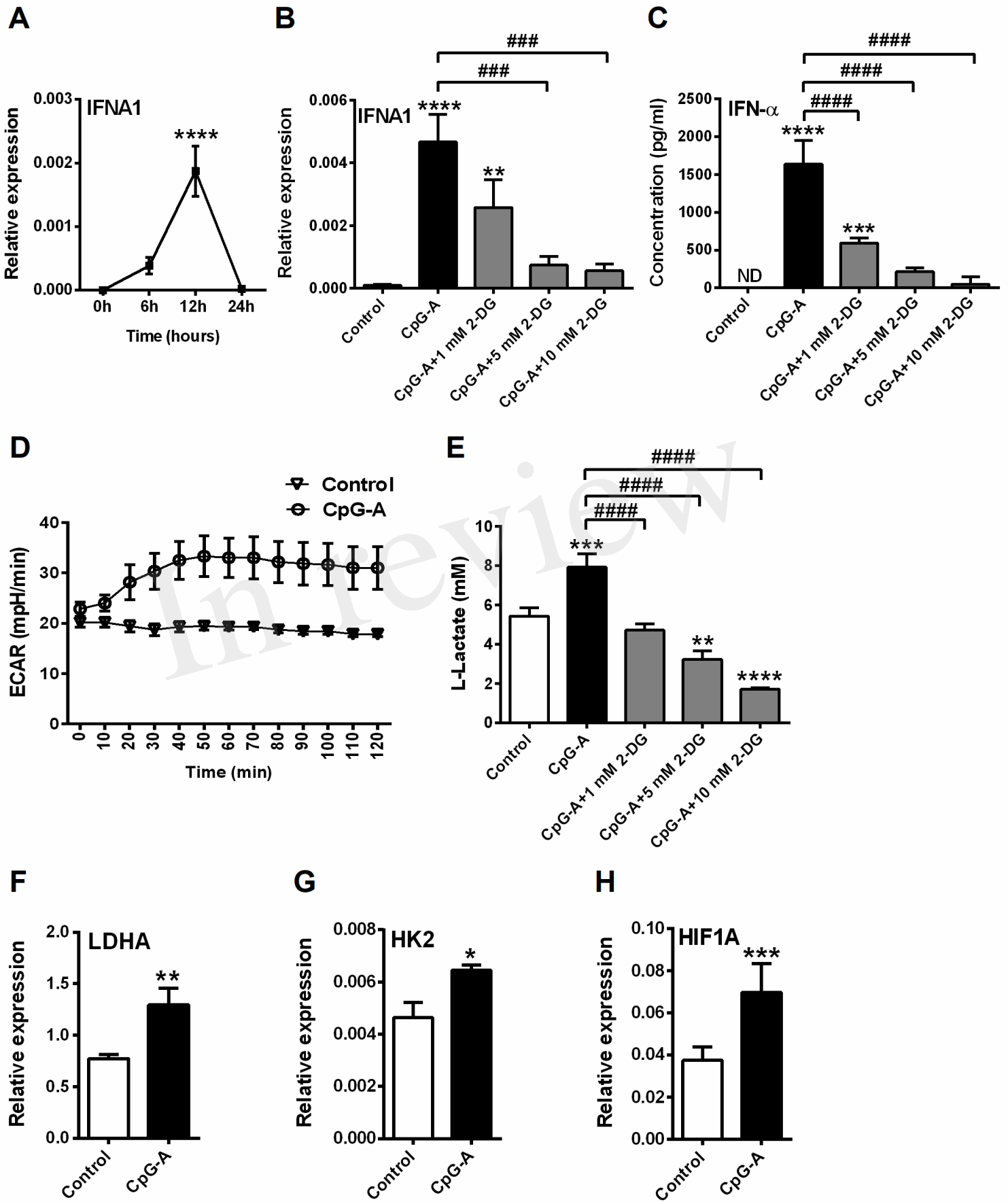


Figure 4.TIF

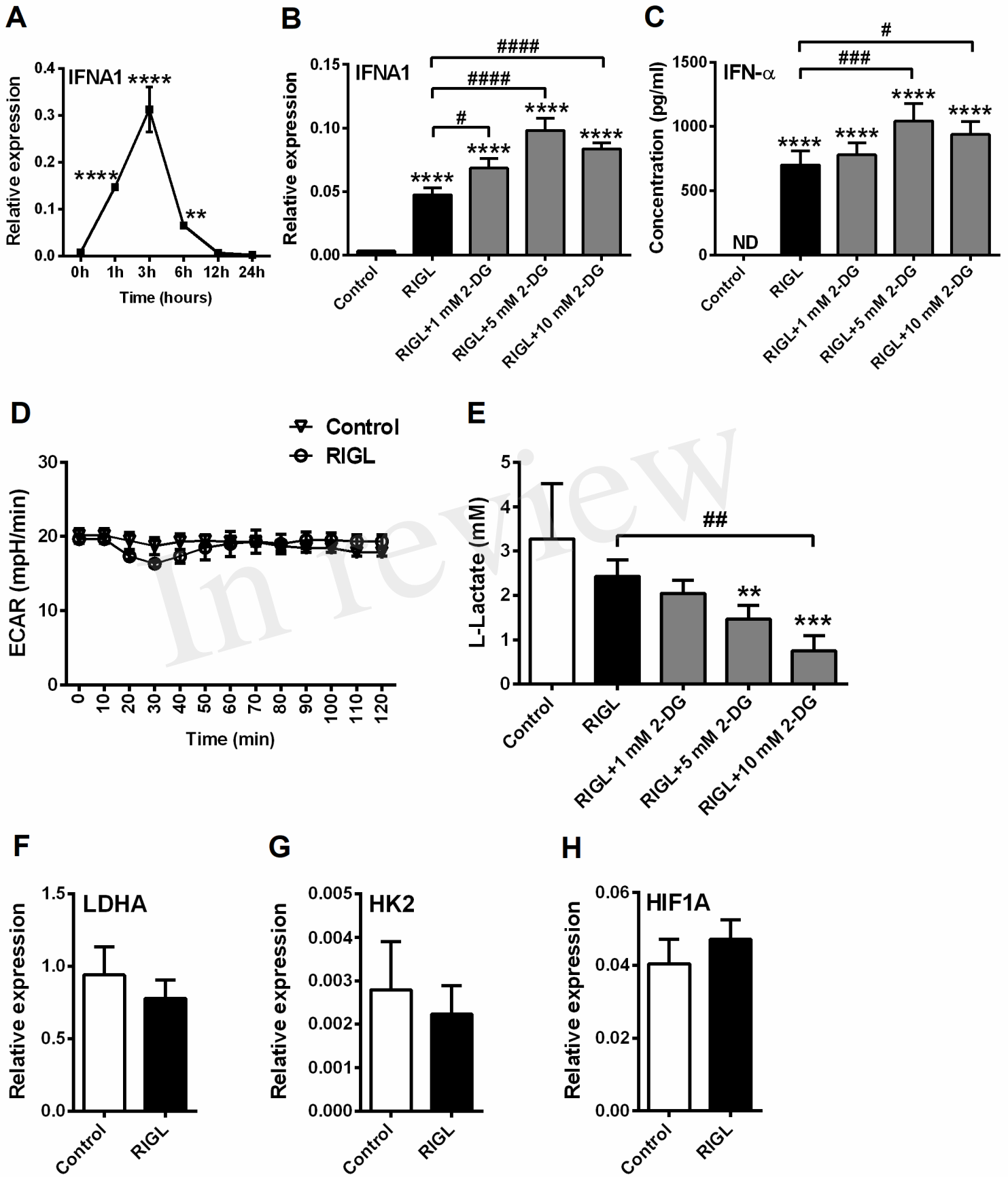


Figure 5.TIF

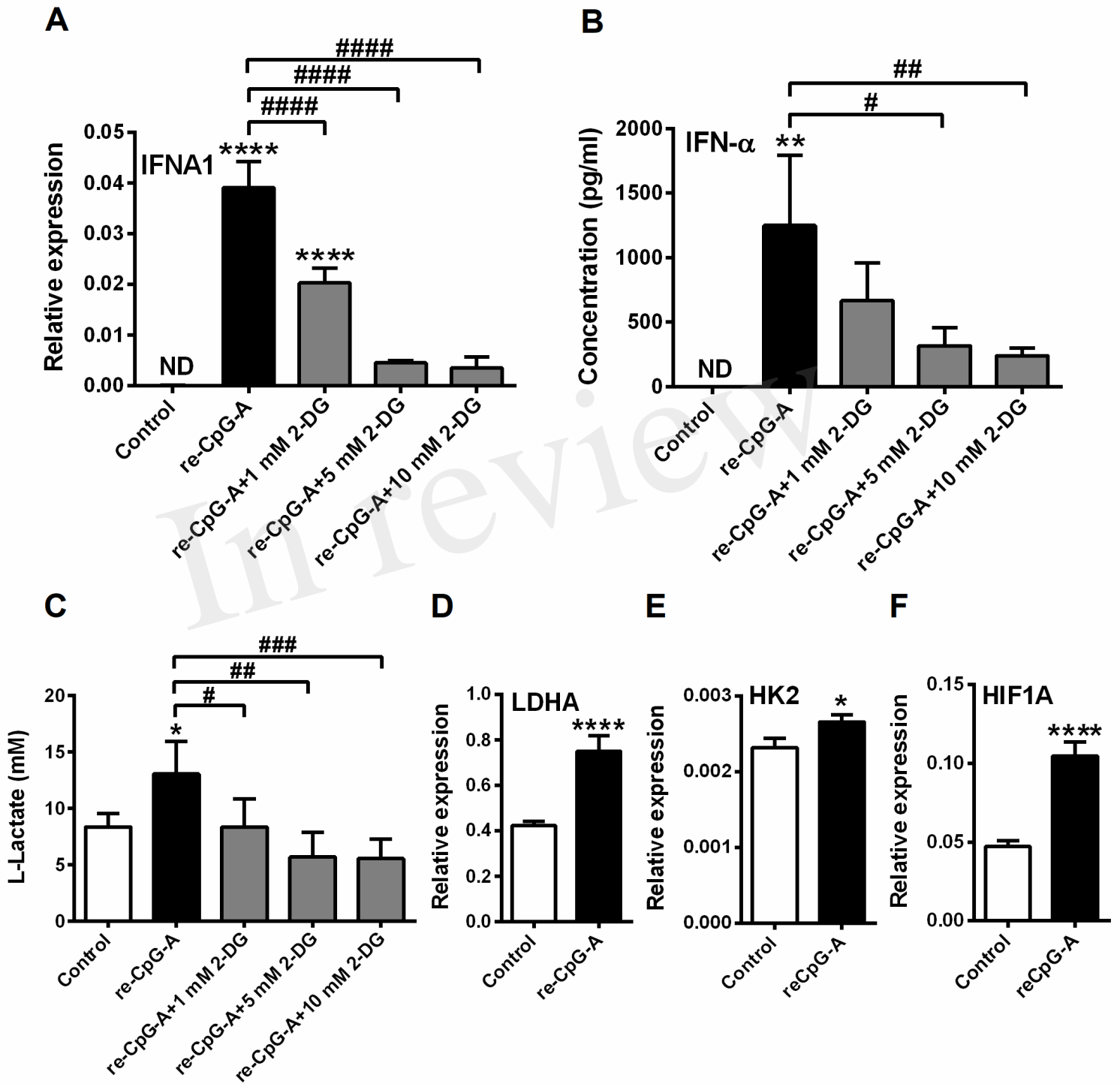


Figure 6.TIF

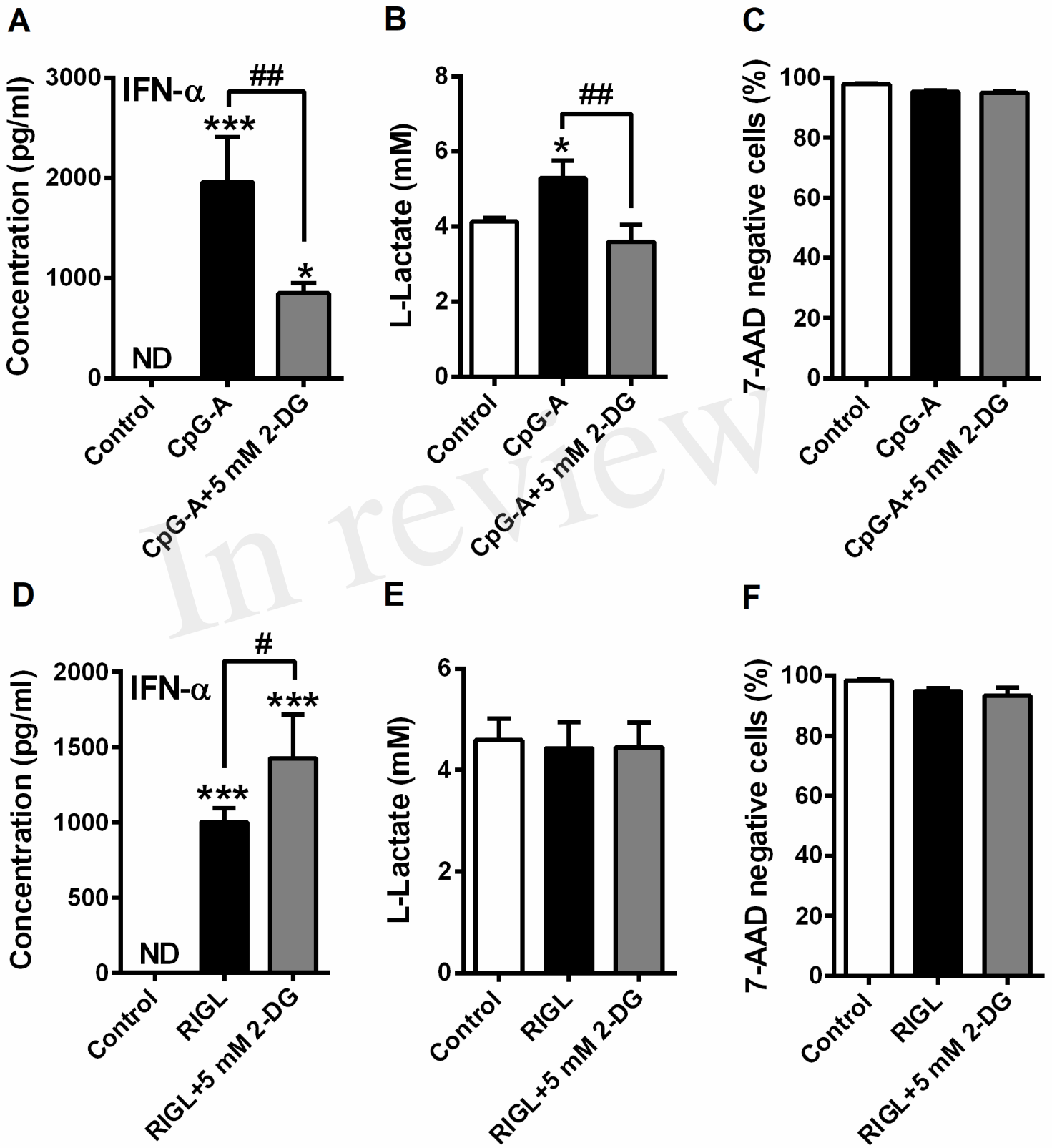


Figure 7.TIF

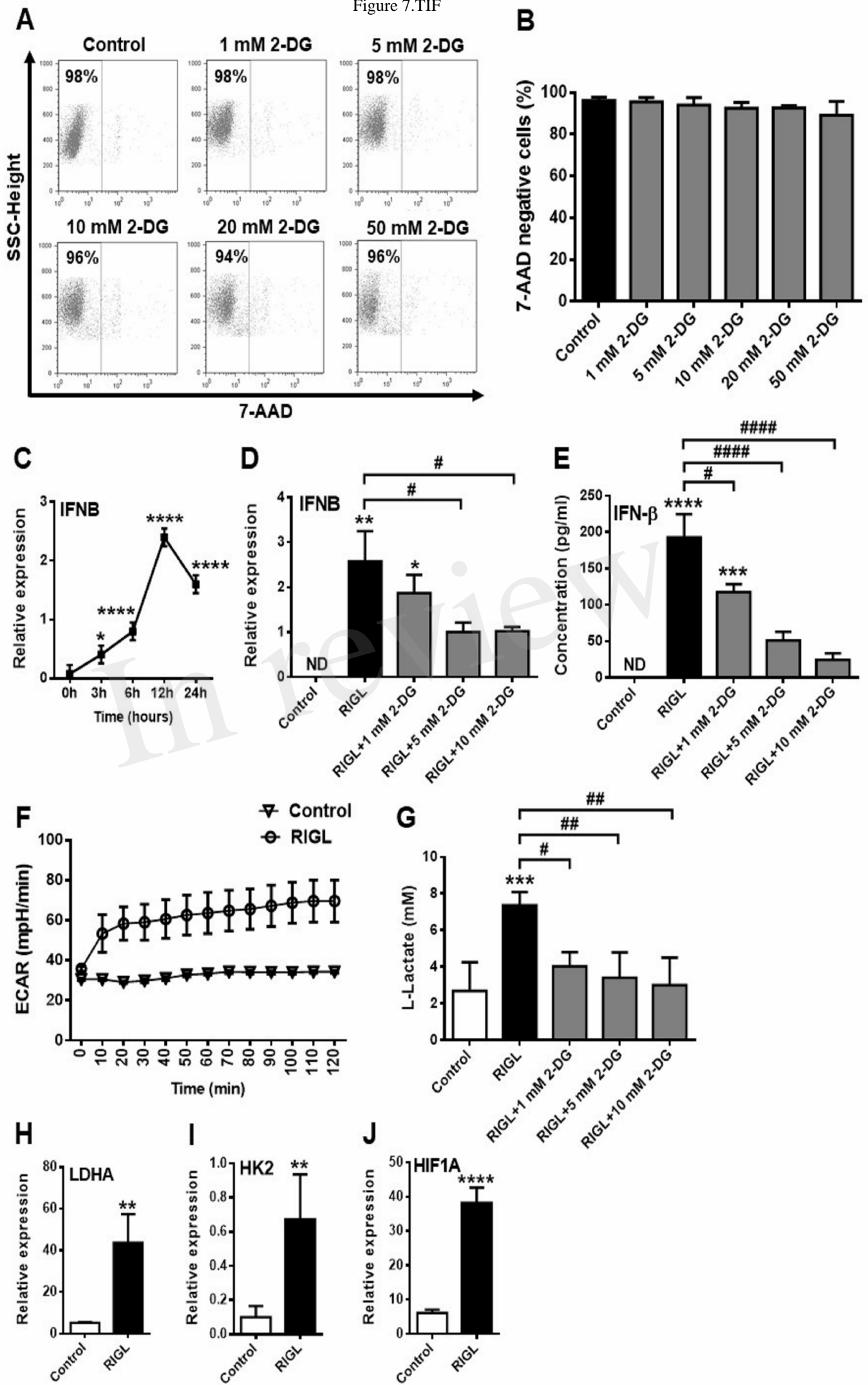
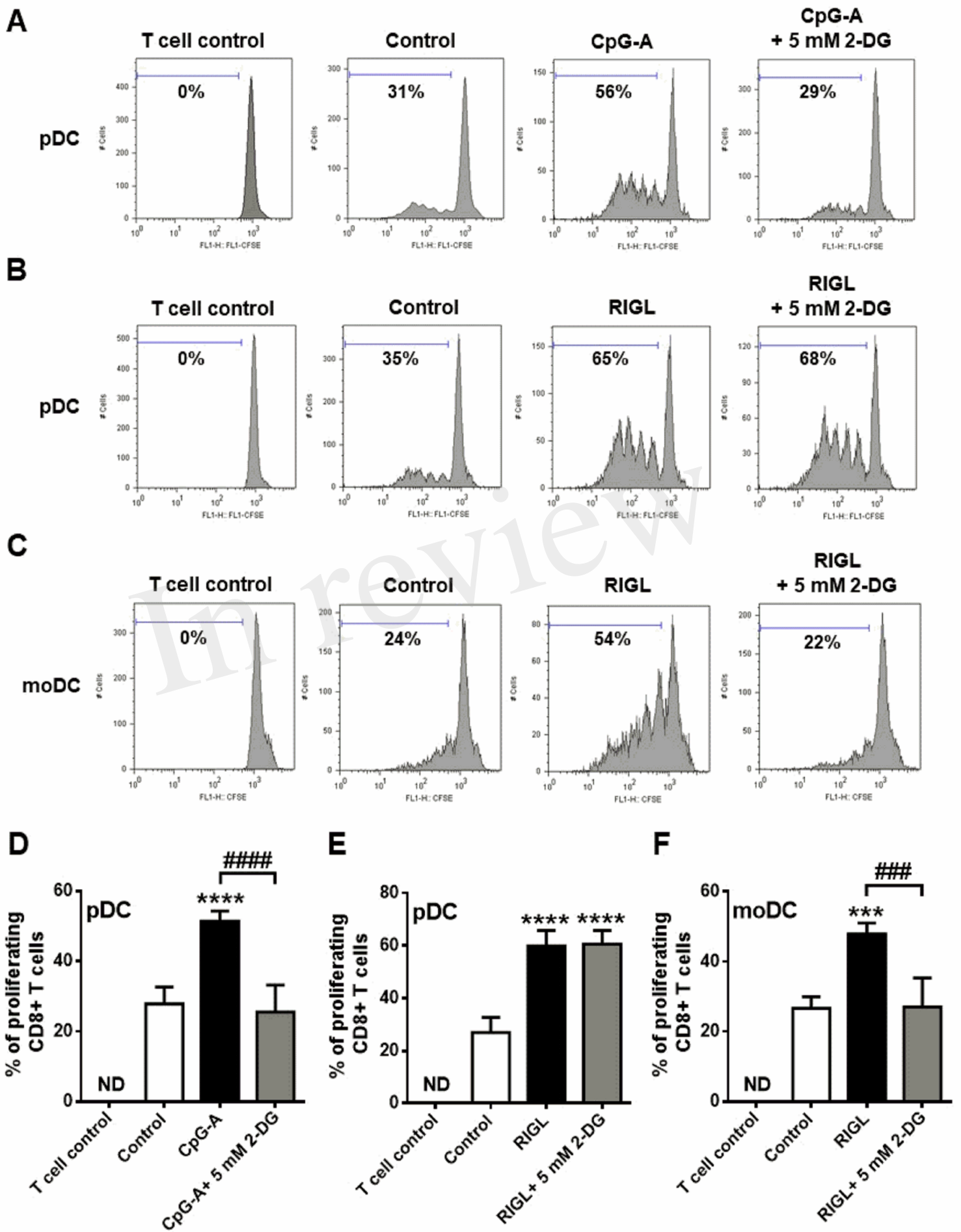


Figure 8.TIF



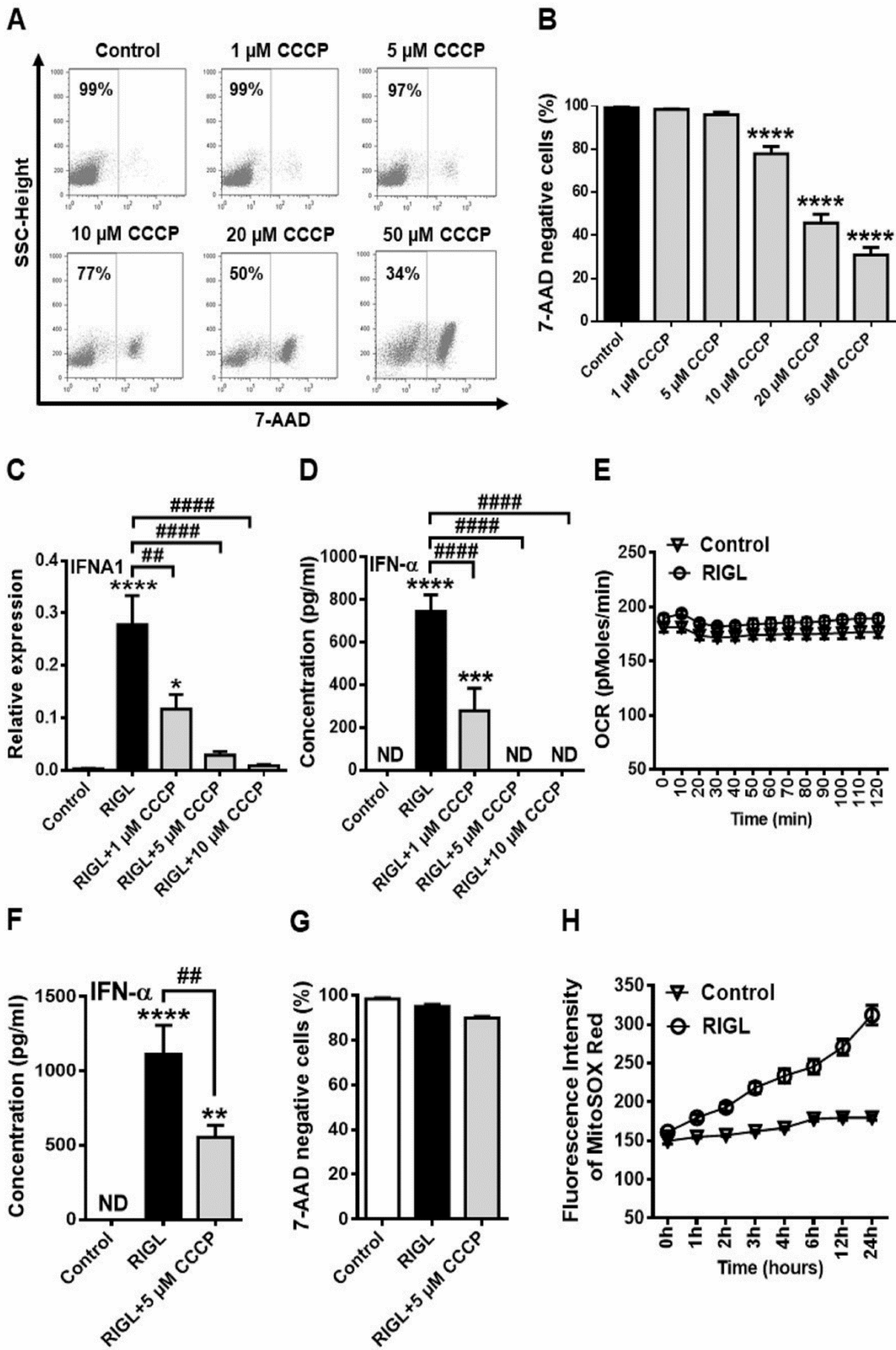
*Supplementary Material*

**Human plasmacytoid and monocyte-derived dendritic cells display distinct metabolic profile upon RIG-I activation**

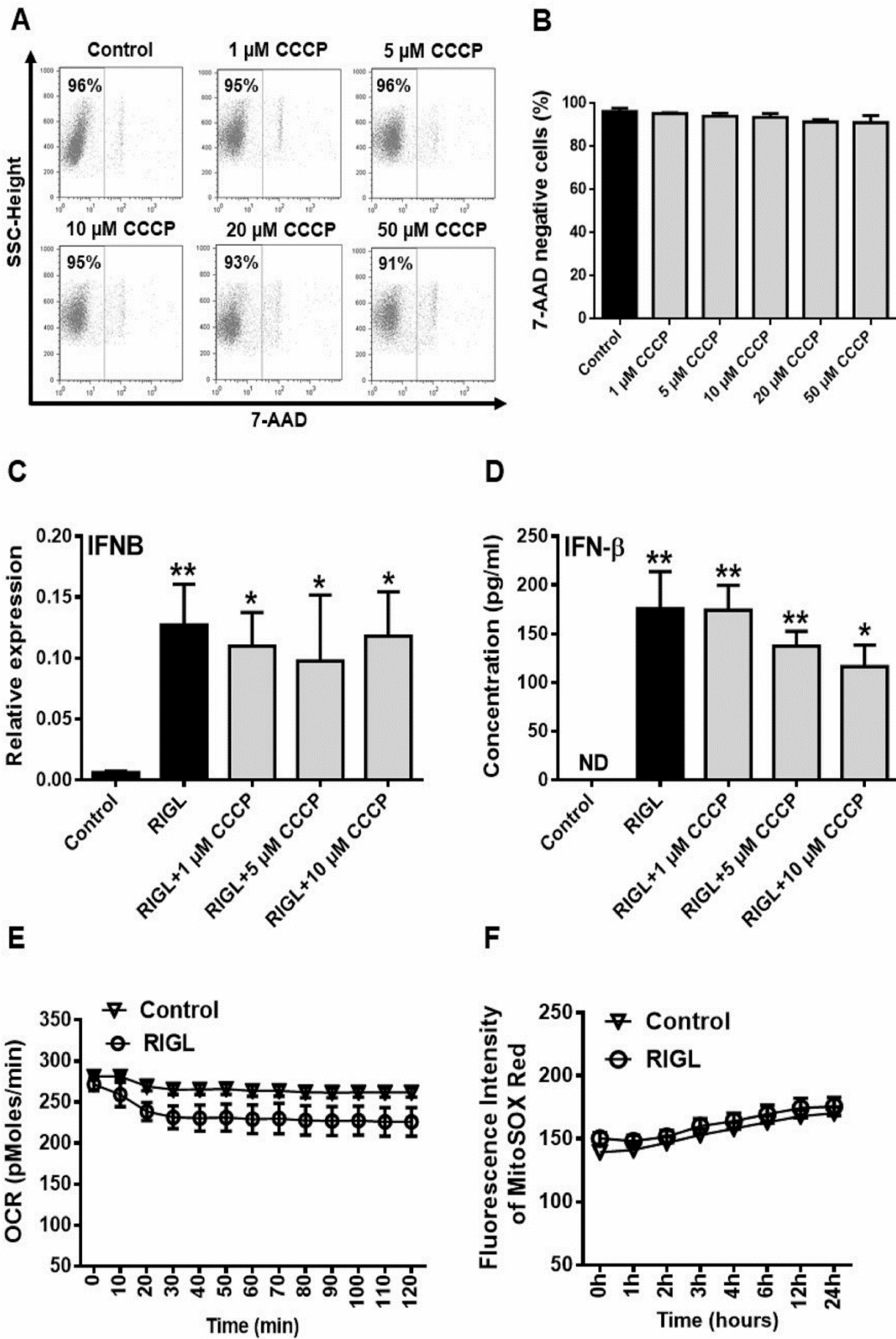
**Tünde Fekete, Mate Sütő, Dora Bencze, Anett Mázló, Attila Szabo, Tamas Biro, Attila Bacsi, Kitti Pazmandi\***

\* **Correspondence:** Kitti Pazmandi: pazmandikitti@yahoo.de

**Supplementary Figures**



**Supplementary Figure 1.** Inhibition of oxidative phosphorylation (OXPHOS) affects the RIG-I-mediated type I IFN production in GEN2.2 cells and in human primary pDCs. **(A,B)** GEN2.2 cells were treated with increasing concentration of mitochondrial uncoupler carbonylcyanide m-chlorophenylhydrazone (CCCP; 1-50  $\mu$ M), then cell viability was analyzed by flow cytometry. **(C,D)** GEN2.2 cells were pre-treated with 0.25  $\mu$ M of CpG-A for 16 hours then following thorough washing steps stimulated with the RIG-I agonist 5'ppp-dsRNA (RIGL, 1  $\mu$ g/ml) in the presence or absence of CCCP (1, 5 and 10  $\mu$ M). The expression of IFN- $\alpha$  was measured at the mRNA level by Q-PCR at 3 hours **(C)** and at the protein level by ELISA at 6 hours **(D)**. **(E)** Following activation with 5'ppp-dsRNA real-time OCR was determined by EFA. The results of a representative experiment are shown. **(F,G)** Primary human pDCs were pre-treated with CpG-A for 16 hours then following thorough washing steps stimulated with the RIG-I agonist 5'ppp-dsRNA in the presence or absence of 5  $\mu$ M CCCP. **(F)** IFN- $\alpha$  protein levels were measured from the supernatants at 6 hours. **(G)** Cell viability was measured by 7-AAD staining using flow cytometry. **(H)** The mtROS production was detected by MitoSOX<sup>TM</sup> Red mitochondrial superoxide indicator. The results of a representative experiment are shown. **(A)** Representative dot plots are shown and numbers indicate the percentage of 7-AAD negative cells. **(B-D,F,G)** Data represent the mean  $\pm$  SD of at least 3 individual experiments. \* $p$ <0.05, \*\* $p$ <0.01, \*\*\* $p$ <0.01, \*\*\*\* $p$ <0.0001 vs. control; # $p$ <0.05, ##### $p$ <0.0001, ND: not determined



**Supplementary Figure 2.** Inhibition of oxidative phosphorylation (OXPHOS) does not affect the viability and RIG-I-mediated type I IFN production in human immature moDCs. **(A,B)** moDCs were treated with increasing concentration of the mitochondrial uncoupler carbonylcyanide m-chlorophenylhydrazone (CCCP; 1-50  $\mu$ M) then cell viability was analyzed by flow cytometry. **(C,D)** Cells were left untreated or stimulated with the RIG-I agonist 5'ppp-dsRNA (RIGL, 1  $\mu$ g/ml) in the presence or absence of CCCP (1, 5 and 10  $\mu$ M). After 12 hours the expression of IFN- $\beta$  was measured at the mRNA level by Q-PCR **(C)** and at the protein level by ELISA **(D)**. **(E)** Following activation with 5'ppp-dsRNA real-time OCR was determined by EFA. The results of a representative experiment are shown. **(F)** The mtROS production was detected using MitoSOX<sup>TM</sup> Red mitochondrial superoxide indicator. The results of a representative experiment are shown. **(A)** Representative dot plots are shown and numbers indicate the percentage of 7-AAD negative cells. **(B-D)** Data represent the mean  $\pm$  SD of at least 3 individual experiments. \* $p$ <0.05, \*\* $p$ <0.01 vs. control, ND: not determined